

UNIVERSIDAD DISTRITAL
FRANCISCO JOSÉ DE CALDAS

Faculty of Mathematical
and Natural Sciences

The Role of the Casimir Effect as a Physical Model for the Organization of Lipid Membranes

Undergraduate thesis submitted in partial fulfillment of the requirements for the degree of Physicist

Yerly Zaudí Gómez Contreras

Academic Program in Physics
Universidad Distrital Francisco José de Caldas

Bogotá, D.C.
July, 2026

The Role of the Casimir Effect as a Physical Model for the Organization of Lipid Membranes

Thesis submitted as a partial requirement for the degree of
Physicist

Modality: Research Internship
Work carried out at the Pontifica Javeriana University

Internal Supervisor
Ph.D. Miguel José Espitia Rico
Universidad Distrital Francisco José de Caldas

External Supervisor
Ph.D. José Alfonso Leyva Rojas
Pontificia Universidad Javeriana

Academic Program in Physics
Faculty of Mathematical and Natural Sciences
Universidad Distrital Francisco José de Caldas

Bogotá D.C., July of 2026

Agradecimientos

Ante todo, quiero agradecer a mis padres por darme la oportunidad de estudiar física y por apoyarme siempre en el camino hacia mis sueños. Todo lo que he logrado es gracias a ellos; han sido una presencia constante y firme en mi vida, y les estoy profundamente agradecida por ello.

También quiero agradecer a mi hermana por cuidarme y apoyarme durante todo este proceso, por sus palabras de aliento y por todo lo demás que me ha brindado a lo largo del camino.

Mi gratitud se extiende asimismo a mi director de tesis, quien, desde las primeras etapas de mi carrera, me ha guiado en el ámbito de la física y ha contribuido a moldear y complementar mi formación como física. Gracias por su paciencia, su tiempo y su dedicación.

A mis compañeros, por todos los años y momentos que hemos compartido.

Por último, mi agradecimiento es para la física, por darme una nueva forma de ver, entender y admirar el mundo; porque, como dijo Tobias Forge en Mary On A Cross: “Your beauty never scared me”.
Gracias a todos.

Resumen

Las membranas biológicas son estructuras esenciales para la vida. En las últimas décadas, se ha propuesto que fenómenos cuánticos, como el efecto Casimir, podrían desempeñar un papel adicional en la organización de estos sistemas a nanoescala. Este trabajo tiene como objetivo evaluar la viabilidad de esta hipótesis, comprendiendo el efecto Casimir como una posible contribución física al comportamiento de las membranas lipídicas. Para ello, se desarrolló primero la cuantización canónica del campo electromagnético, estableciendo el marco teórico necesario para calcular la energía del vacío. Posteriormente, se derivó la fuerza de Casimir para dos configuraciones geométricas: placas planas paralelas y esferas concéntricas, utilizando técnicas de regularización y renormalización para abordar las discrepancias inherentes en el cálculo. Finalmente, se analizó la plausibilidad física de aplicar estos resultados al contexto biológico comparando la magnitud y la dependencia de la distancia de la fuerza de Casimir con otras interacciones de membrana conocidas. Los resultados muestran que, si bien ambas geometrías producen expresiones consistentes, el comportamiento resultante es monótono, careciendo de puntos de equilibrio o mínimos de energía que expliquen por qué la membrana se estabiliza en su espesor característico. Se concluye que la representación de placas plano-paralelas es suficiente como primera aproximación, dado que la corrección de curvatura es insignificante a escala celular, y que el efecto Casimir constituye un modelo geométricamente plausible, aunque todavía exploratorio, para complementar la comprensión física de la organización de la membrana lipídica.

Keywords: Efecto Casimir, membranas lipídicas, viabilidad, cuantización del campo electromagnético.

Abstract

Biological membranes are essential structures for life. In recent decades, it has been proposed that quantum phenomena, such as the Casimir effect, could play an additional role in the organization of these systems at the nanoscale. This work aims to evaluate the feasibility of this hypothesis by understanding the Casimir effect as a possible physical contribution to the behavior of lipid membranes. To this end, the canonical quantization of the electromagnetic field was first developed, establishing the necessary theoretical framework for calculating the vacuum energy. Subsequently, the Casimir force was derived for two geometric configurations: parallel flat plates and concentric spheres, using regularization and renormalization techniques to address the inherent discrepancies in the calculation. Finally, the physical plausibility of applying these results to the biological context was analyzed by comparing the magnitude and distance dependence of the Casimir force with other known membrane interactions. The results show that, while both geometries produce consistent expressions, the resulting behavior is monotonous, lacking equilibrium points or energy minima that would explain why the membrane stabilizes at its characteristic thickness. It is concluded that the planar-parallel plate representation is sufficient as a first approximation, given that curvature correction is negligible at the cellular scale, and that the Casimir effect constitutes a geometrically plausible, albeit still exploratory, model to complement the physical understanding of lipid membrane organization.

Keywords: Casimir effect, lipid membranes, viability, quantization of the electromagnetic field.

Contents

Acknowledgments iii

Abstract iv

Abstract v

1 Introduction 1

1.1 Objectives . . . 2
1.1.1 General Objective . . . 2
1.1.2 Specific Objectives . . . 2
1.2 Work Plan . . . 2
1.2.1 Phase I. Theoretical Foundation. . . . 2
1.2.2 Phase II. Casimir Effect. . . . 2
1.2.3 Phase III. Application to Biological Membranes. . . . 3
1.2.4 Bibliometric Analysis and Research Gap . . . 3

2 Canonical Quantization of the Electromagnetic Field 5

2.1 Second Quantization . . . 5
2.1.1 Creation and Annihilation Operators . . . 6
2.2 Quantum Harmonic Oscillator . . . 7
2.3 Quantization of the Electromagnetic Field . . . 10
2.3.1 Gauge Transformation . . . 11
2.3.2 Coulumb Gauge . . . 12
2.3.3 Normal modes and Fourier decomposition . . . 12
2.3.4 Energy of the Electromagnetic Field . . . 18

3 Casimir Effect 21

3.1 Parallel plane plates . . . 21
3.1.1 Boundary conditions and permitted modes . . . 22
3.1.2 Zero-point energy . . . 24
3.1.3 Regularization . . . 26
3.1.4 Casimir's Energy and Force . . . 30
3.2 Two Concentric Spheres . . . 31
3.2.1 Boundary Conditions . . . 33
3.2.2 Regularization Method . . . 37

4 The Lipid Membrane as a Boundary System for the Casimir Effect 40
4.1 Biological Membranes 40
4.2 Lipid Membranes 41
4.2.1 Membrane Potential 41
4.2.2 Equivalent electrical circuit for a biological membrane 42
4.3 Viability of the Casimir effect 43
4.3.1 Transverse compressibility modulus 45
Bibliography 49

List of Figures

1.1 Thematic cluster 3
1.2 Overlay Visualization 4

2.1 In the classical regime, a particle with a fixed total energy E is strictly confined within the potential well $V(x)$. The parameters $-x_M$ and x_M represent the classical inflection points, which define the maximum amplitude of the oscillation where the kinetic energy is identically zero $V(x) = \frac{1}{2}m\omega^2x^2$, within which a classical particle would exhibit a continuous range of permissible energy states. In contrast, the left-hand side shows the quantum-mechanical scheme, where the allowed energy states are restricted to a discrete, equidistant sequence of horizontal levels indexed by the non-negative integer n.Source: Own elaboration 10
2.2 . The electromagnetic field is confined to a box 13
2.3 Polarization vectors and illustration of k-space 14

3.1 Subtraction of zero-point energies. 23
3.2 Behavior Casimir's Energy and Force for two parallel plane plates . . . 31
3.3 Geometry representation of the system, two concentric spheres of radius a and b, qith a sepatation distance d. 32
3.4 Behavior of the Besse Funtions of the First kind 34
3.5 Behavior of the Besse Funtions of the Second kind. 34
3.6 Casimir energy and associated pressure for a spherical geometry. Dependence of the Casimir energy $E_C(d)$ (left, in nJ) and Casimir pressure $P_C(d)$ (right, in Pa) on the separation distance d ranging from 1.5 nm to 10 nm. The geometric parameters were set to $a \approx 10\ \mu\text{m} - 5$ nm) and $b = 10\ \mu$m. Both magnitude curves exhibit the characteristic attractive (negative) behavior of the Casimir force, increasing nonlinearly as the separation approaches sub-10 nm regimes. A reference distance $d_{\text{ref}} = 5$ nm is highlighted by the vertical dashed line. 39

4.1 Schematic representation of a biological membrane with a lipid bilayer. Retrieved from: `https://biomodel.uah.es/model2/lip/membranas-func.htm` 40

4.2 General structure of a dipalmitoylphosphatidylcholine molecule. The polar head is composed of a choline group attached to a phosphate, while the hydrophobic region corresponds to two long hydrocarbon chains, which constitute the lipid "tails." Source: Author's own work 41
4.3 Compartment separated by a membrane where ions are driven from 2 to 1 as a result of chemical and electrical power differences. Source: Own elaboration 42
4.4 Diagram of a cell membrane and its equivalent circuit. a) The lipid bilayer acts as a charge storage device, like a capacitor. b) Model of a membrane and transport protein, where the capacitor represents the membrane, and the resistance (R) models the ionic conductance due to the transport channels. Source: Author's own work 43
4.5 Comparison between Casimir pressure and Hamaker pressure 46

List of Tables

3.1 Chronological summary of Casimir effect experiments: geometry, technique, and uncertainty. 22

1

Introduction

This undergraduate thesis was developed during an external internship within the framework of the mobility agreement between the Francisco José de Caldas District University and the Pontifical Javeriana University. The cell membrane is a complex and dynamic structure, essential for life; it acts as a barrier that prevents the cell's contents from escaping, but at the same time allows the selective entry of substances. This type of membrane is widely studied in its bilayer configuration, formed mainly by molecules called lipids, which have a hydrophilic head and one or two hydrophobic tails [1]. Traditionally, the interactions that govern these structures have been attributed to hydrophobic, electrostatic, and van der Waals forces [2].

However, in recent decades, a different perspective has emerged, suggesting that phenomena from the quantum world, such as the Casimir effect, could play a relevant role in the organization of biological systems at the nanoscale [3, 4]. The Casimir effect, predicted in 1948 by Hendrik Casimir, states that placing two perfectly conducting, neutral, and parallel plates in a vacuum alters the zero-point energy of the electromagnetic field, generating an attractive force between them. While this force is very weak at macroscopic distances, it becomes significant at nanometer distances, corresponding to the characteristic length range of lipid membranes[5].

In this context, the central hypothesis of this work is that quantum vacuum boundary effects can contribute significantly to understanding certain aspects of lipid membrane organization, particularly in lipid bilayers. To explore this hypothesis, this work is structured in three phases. First, the mathematical formalism of electromagnetic field quantization will be established, laying the groundwork for calculating vacuum energy. Second, the Casimir force will be understood and calculated for two geometric configurations: parallel flat plates and concentric spheres. Finally, the plausibility of these forces being relevant in the biological context will be discussed, comparing their magnitude and dependence on distance with other known forces and analyzing the implications for membrane organization.

1.1 Objectives

1.1.1 General Objective

To understand the Casimir effect and its relationship to biological membranes.

1.1.2 Specific Objectives

- Derive the quantization of the electromagnetic field in a vacuum.
- Reproduce the Casimir force for a system of parallel plates.
- Reproduce the Casimir force for a configuration of spherical caps.
- Understand the equivalence between the Casimir effect and a biological membrane.

1.2 Work Plan

The development of this work is planned in three thematic phases:

1.2.1 Phase I. Theoretical Foundation.

A literature review will be carried out in order to establish a formal analysis of the methods for quantizing the electromagnetic field, thus obtaining the necessary conceptual basis for its application in calculating the Casimir effect.

Topics to be addressed:

- Review of Maxwell's Equations.
- Method of quantizing the electromagnetic field.
- Creation and annihilation operators.
- Second quantization

1.2.2 Phase II. Casimir Effect.

The problem will be addressed using regularization and renormalization techniques, as well as the implementation of boundary conditions for the quantized electromagnetic field.

Topics to be covered:

- Implementation of boundary conditions for the quantized electromagnetic field.

- Regularization and renormalization.
- Casimir force on parallel plates.
- Casimir force on spherical caps.

1.2.3 Phase III. Application to Biological Membranes.

Finally, a review of recent work in biophysics will be conducted to compare the results obtained in the calculation of Casimir forces with the interactions observed in biological membranes.

1.2.4 Bibliometric Analysis and Research Gap

With the aim of identifying scientific production on the application of the Casimir effect as a model in biological membranes, a bibliographic search was carried out in the Scopus database using the search equation "Casimir effect" AND "membrane", subsequently the following maps were created through VOSviewer:

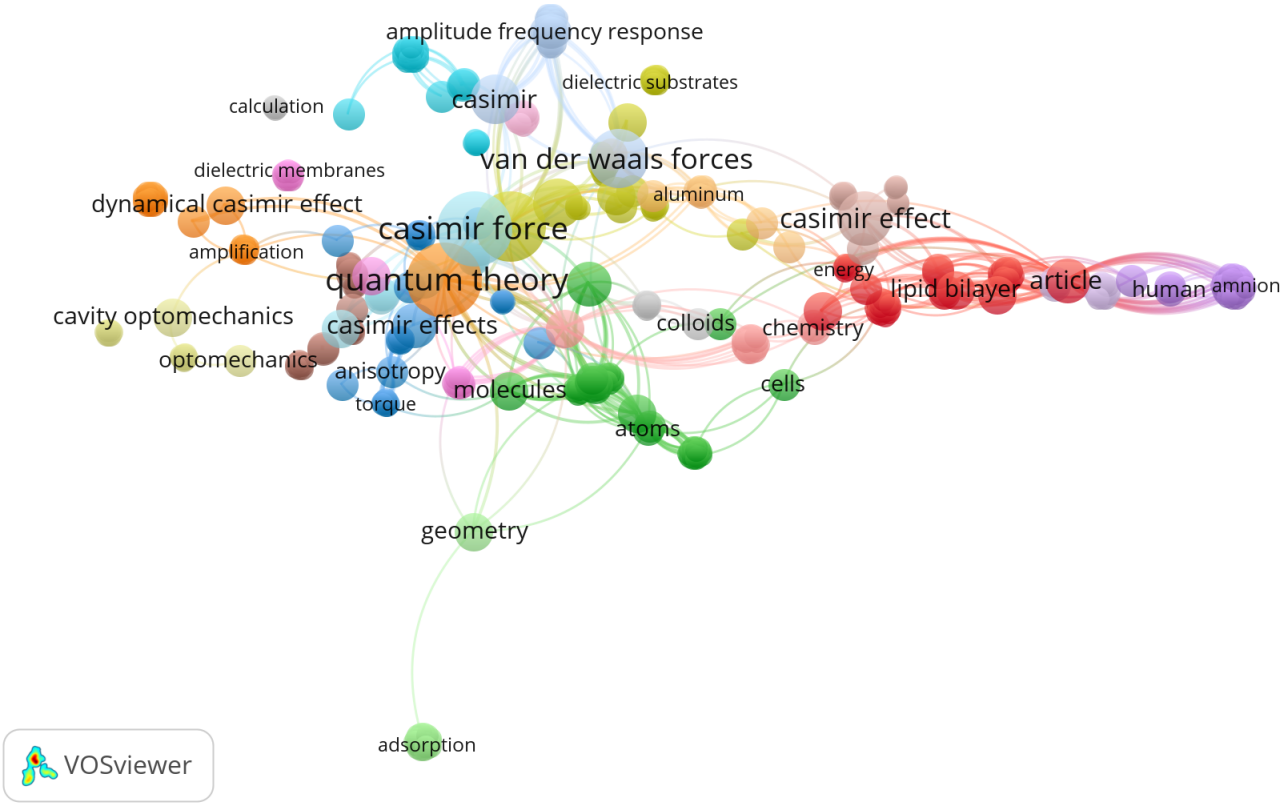


Figure 1.1: Thematic cluster

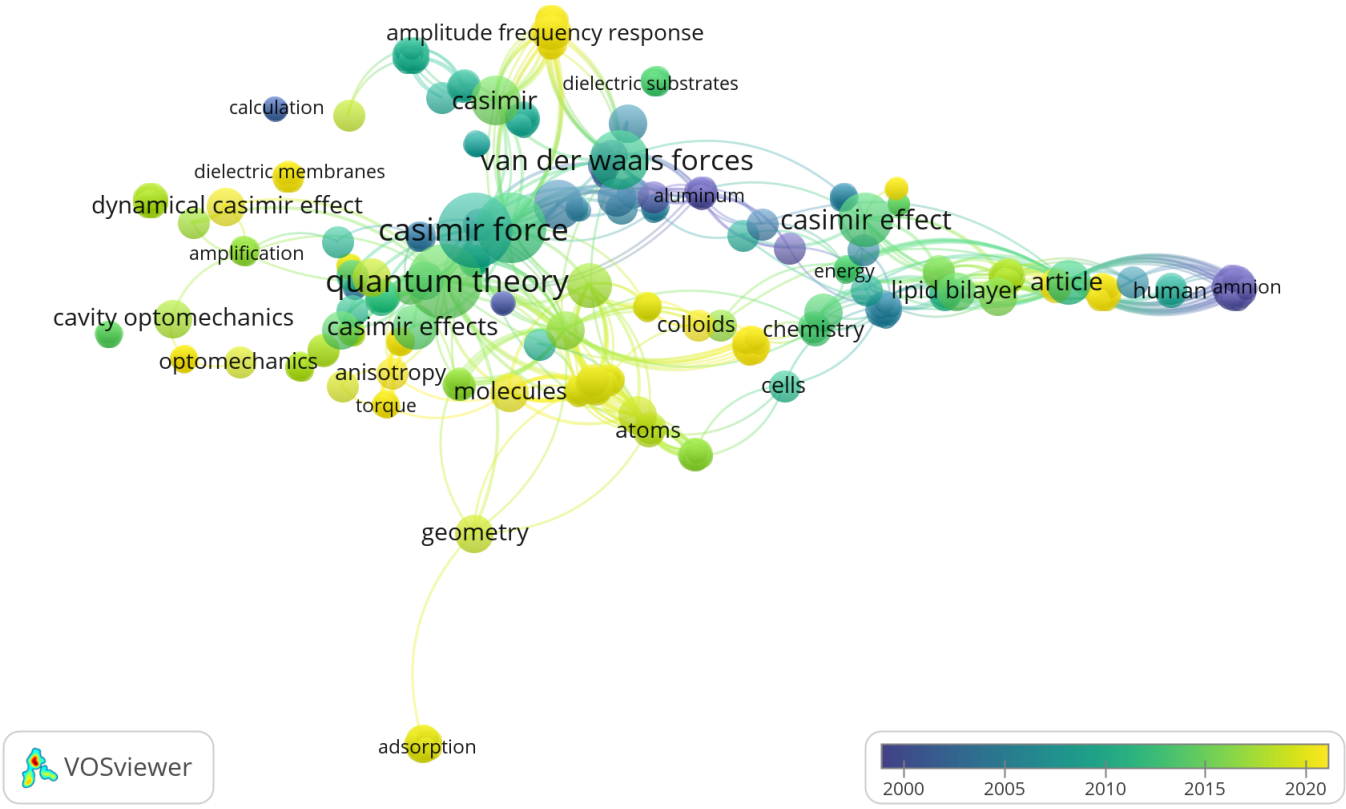


Figure 1.2: Overlay Visualization

Figure 1.1 bis shows a color-coded visualization grouping research areas. Our node of interest is "lipid bilayer," located on the periphery near "energy," "chemistry," "colloids," "cells," "human," and "amnion," with only three occurrences and 63 links. This suggests that it is always discussed alongside the same terms and not as an autonomous topic. In fact, a search of the bibliography identified only one article addressing this applicability. In Fig.1.2, we note that the nodes have a green-yellow color, indicating that the publications linking "lipid bilayer" to the rest of the network are from a relatively recent period, approximately 2014-2018.

2

Canonical Quantization of the Electromagnetic Field

2.1 Second Quantization

In 1927, Dirac laid the foundations of a systematic quantum theory of fields in his famous paper "The Quantum Theory of the Emission and Absorption of Radiation". The quantization of the electromagnetic field extends naturally to the quantization of any classical field. This formalism is important as it allows us to consider the possibility that the number of particles may change [6, 7]. The starting point is a change of basis. Let $\{|\phi_k\rangle\}_{k\in\mathbb{N}}$ be a complete orthonormal basis of the single-particle Hilbert space $\mathcal{H}_1$. Instead of specifying which particle occupies which orbital, the state of the system is described by occupation numbers.

$$|n_1, n_2, ..., n_k\rangle$$

Where n_k is the number of particles in the mode $\{|\phi_k\rangle\}$. For bosons, $n_k \in \mathbb{N}$; for fermions, the Pauli exclusion principle restrict, $n_k \in \{0, 1\}$. This basis must be complete and orthonormal.

$$\langle n'_1, n'_2, ..., n'_\infty | n_1, n_2, ..., n_\infty \rangle \qquad \text{Orthogonality}$$

$$\sum_{n_1,n_2,...,n_k} |n_1, n_2, ..., n_\infty\rangle \langle n_1, n_2, ..., n_\infty| = 1 \qquad \text{Completeness}$$

This vector is a member of a new kind of vector space, called "Fock space", Which is built as the direct sum of all subspaces of N-particule with appropriate symmetrization [8, 9].

Fock Space

Is the direct sum of the tensor products of all N-particle Hilbert spaces:

$$\mathcal{F}_\nu(\mathcal{H}) = \bigoplus_{n=0}^{\infty} S_\nu^{(n)} \mathcal{H}^{\otimes n} \tag{2.1}$$

Where ν is $+$ for bosons and $-$ for fermions.

2.1.1 Creation and Annihilation Operators

The creation and annihilation operators are mathematical operators introduced to add and remove a particle from a many-body system. It is worth noting that Paul Dirac introduced these operators in his influential 1927 paper [6], using the notation b_r and b_r^*, but in modern quantum field theory these correspond to $a_j^\dagger$ (creation) and a_i (annihilation). For bosons, the following commutation rules apply:

$$[a_i, a_j^\dagger] = a_i a_j^\dagger - a_j^\dagger a_i = \delta_{ij} \tag{2.2}$$

$$[a_j^\dagger, a_j^\dagger] = [a_i, a_i] = 0 \tag{2.3}$$

The number operator is also defined:

$$N = \sum_i n_i = \sum_i a_i^\dagger a_i \tag{2.4}$$

Since field modes commute with each other, we can analyze the eigenvalue spectrum of a single arbitrary mode without loss of generality. For brevity, we will temporarily omit the mode indices i, j in the following derivation.

$$[N, a] = [a^\dagger a, a] = a^\dagger [a, a] + [a^\dagger, a] a = -a \tag{2.5}$$

$$[N, a^\dagger] = [a^\dagger a, a^\dagger] = a^\dagger [a, a^\dagger] + [a^\dagger, a^\dagger] a = a^\dagger \tag{2.6}$$

The properties of the operators a and $a^\dagger$ on $|n\rangle$ are presented below:

$$\begin{aligned} Na\,|n\rangle &= (aN - a)\,|n\rangle \\ &= aN\,|n\rangle - a\,|n\rangle \\ &= a(n\,|n\rangle) - a\,|n\rangle \\ &= na\,|n\rangle - a\,|n\rangle \\ &= (n-1)a\,|n\rangle \end{aligned}$$

$$\begin{aligned} Na^\dagger |n\rangle &= (a^\dagger N + a^\dagger) |n\rangle \\ &= a^\dagger N |n\rangle + a^\dagger |n\rangle \\ &= a^\dagger (n |n\rangle) + a^\dagger |n\rangle \\ &= n a^\dagger |n\rangle + a^\dagger |n\rangle \\ &= (n+1) a^\dagger |n\rangle \end{aligned}$$

Therefore, $a |n\rangle$ is a eigenstate of N with eigenvalue $n-1$ and $a^\dagger |n\rangle$ is a eigenstate of N with eigenvalue $n+1$:

$$\begin{aligned} a |n\rangle &= c_n |n-1\rangle \\ a^\dagger |n\rangle &= c_n |n+1\rangle \end{aligned}$$

Where c_n is a normalization constant.

$$\langle n| a^\dagger a |n\rangle = |c^2| \tag{2.7}$$

Now, since $a^\dagger a$ is just the number operador, we can evaluate the left-hand side of (2.7), so

$$n = |c|^2 \tag{2.8}$$

c is taken as real and positive by convention, thus we obtain the final normalized action of the ladder operators:

$$a |n\rangle = \sqrt{n} |n-1\rangle \tag{2.9}$$

$$a^\dagger |n\rangle = \sqrt{n+1} |n+1\rangle \tag{2.10}$$

These results reveal that the $\sqrt{n}$ factor enforces a lower bound on the spectrum since $a |0\rangle = 0$, preventing states with negative eigenvalues on account of the positivity requirement for the norm. Conversely, the $\sqrt{n+1}$ coefficient guarantees rasequence can be applied indefinitely, yielding an infinite tower of discrete energy eigenstates characterized by non-negative integers ($n \geq 0$) [8, 10, 11].

Ladder Operators

While creation and annihilation operators create and destroy particles, ladder operators are unique to the quantum harmonic oscillator; their function is to lower and raise a particle's energy level.

2.2 Quantum Harmonic Oscillator

This is a fundamental problem, as it is one of the few quantum mechanical systems that can be treated with precision. Therefore, it plays a significant role in numerous quantum mechanical systems, for example; in the description of a set of identical particles which

are in the same state. Furthermore, its relevance can be seen in comments in the literature such as: "...the current form of quantum mechanics is largely a physics of harmonic oscillators" [9]. Additionally, its quantization in terms of ladder-opperators points the direction of the quantization of field theories[12, 13, 14]. This system is the quantum analogue of the classical harmonic oscillator. Since a arbitrary smooth potential in the vicinity of a stable equilibrum point. The first quantization in physics refers to the property of particles that certain operators do not commute [10]:

$$[x, p_x] = i\hbar \tag{2.11}$$

Let us consider an arbitrary potential $V(x)$ expanded in a Taylor series around the equilibrium point:

$$V(x) = \sum_{j=0}^{\infty} \frac{\partial^j V(x_0)}{\partial x_0^j}(x - x_0)^j \approx \frac{1}{2}\frac{\partial^2 V(x_0)}{\partial x_0^2}(x - x_0)^2$$

Where $\frac{\partial^2 V(x_0)}{\partial x_0^2}$ acts like the spring constant in a clasical mechanical oscillator, so the potential is

$$V(x) = \frac{1}{2}m\omega^2 x^2 \tag{2.12}$$

About the terms of the Taylor series

Terms that are not of second order are eliminated because the zeroth order term is a constant displacement of no interest, the first order term is zero at the equilibrium point, and the higher-order terms are negligible [15].

The hamiltonian, which we use in the present treatment, is

$$H = \frac{p^2}{2m} + \frac{1}{2}m\omega^2 x^2 \tag{2.13}$$

For quantization, x and p are promoted to opertors:

$$x \to \hat{x} = x \tag{2.14}$$

$$p \to \hat{p} = i\hbar\frac{d}{dx} \tag{2.15}$$

$$H = \frac{\hat{p}^2}{2m} + \frac{1}{2}m\omega^2 \hat{x}^2 \tag{2.16}$$

Mathematically, the Hamiltonian of the quantum harmonic oscillator is fundamentally structured as a sum of quadratic operators. The central strategy of the algebraic approach is to exploit this characteristic through a canonical transformation that factors

the Hamiltonian into a product of non-Hermitian operators. This procedure systematically shifts the problem of the eigenvalues of the original coordinate and momentum representation to the task of diagonalizing a new operator, whose well-defined algebraic properties drastically simplify the determination of the energy spectrum[15].

$$x^2 + p^2 = (x + ip)(x - ip) = |z|^2 = z^* z$$

the forms of the operators is then

$$\hat{a} = \sqrt{\frac{m\omega}{2\hbar}}\Big(\hat{x} + \frac{i\hat{p}}{m\omega}\Big), \qquad \hat{a}^\dagger = \sqrt{\frac{m\omega}{2\hbar}}\Big(\hat{x} - \frac{i\hat{p}}{m\omega}\Big) \tag{2.17}$$

$\hat{x}$ and $\hat{p}$ can be expressed in terms of $\hat{a}$ and $\hat{a}^\dagger$

$$\hat{x} = \sqrt{\frac{\hbar}{2m\omega}}(\hat{a} + \hat{a}^\dagger), \qquad \hat{p} = -i\sqrt{\frac{\hbar}{2m\omega}}(\hat{a} - \hat{a}^\dagger) \tag{2.18}$$

Putting this in the Hamiltonian

$$H = \frac{1}{2m}\Big(-\frac{m\omega\hbar}{2}(\hat{a} - \hat{a}^\dagger)^2\Big) + \frac{1}{2}m\omega^2\Big(\frac{\hbar}{2m\omega}(\hat{a} + \hat{a}^\dagger)^2\Big)$$

Using Eqs. (2.2), (2.3), and (2.4)

$$H = \hbar\omega\Big(\hat{N} + \frac{1}{2}\Big) \tag{2.19}$$

Since H is simply a linear function of N, N can be diagonalized simultaneously with H. We denote an energy eigenstate of N by its eigenvalue n, so

$$N\,|n\rangle = n\,|n\rangle \tag{2.20}$$

$$H\,|n\rangle = \Big(n + \frac{1}{2}\Big)\hbar\omega\,|n\rangle \tag{2.21}$$

Consequently, the energy eigenvalues are given by

$$E_n = \Big(n + \frac{1}{2}\Big)\hbar\omega \tag{2.22}$$

With $n = 0, 1, 2, 3...$, the energy levels are equally spaced over the interval $\hbar\omega$. It is important to note that the ground state energy is not zero, but $\hbar\omega/2$. The harmonic oscillator also plays a role in the study of the electromagnetic field. This can be expanded according to the normal modes of a cavity, and, using Maxwell's equations, it can be shown that each of the coefficients of this expansion obeys a differential equation in the form of the harmonic oscillator[14].

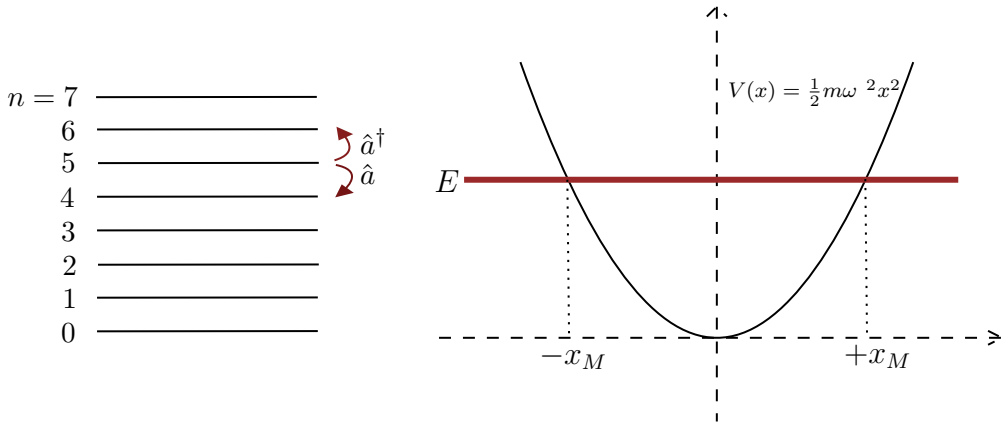


Figure 2.1: In the classical regime, a particle with a fixed total energy E is strictly confined within the potential well $V(x)$. The parameters $-x_M$ and x_M represent the classical inflection points, which define the maximum amplitude of the oscillation where the kinetic energy is identically zero $V(x) = \frac{1}{2}m\omega^2x^2$, within which a classical particle would exhibit a continuous range of permissible energy states. In contrast, the left-hand side shows the quantum-mechanical scheme, where the allowed energy states are restricted to a discrete, equidistant sequence of horizontal levels indexed by the non-negative integer n.Source: Own elaboration

2.3 Quantization of the Electromagnetic Field

The excitation state produced in space by the presence of electric charges constitutes an electromagnetic field. This field is represented by two vector fields, **E** and **B**, called the electric field and magnetic induction, respectively. When working in a vacuum and in the absence of free sources ($\rho = 0$ and $\mathbf{j} = 0$), Maxwell's equations, which govern classical electromagnetic phenomena and serve as the starting point for field quantization [16, 17, 18], are expressed as:

$$\nabla \cdot \mathbf{E} = 0 \tag{2.23}$$

$$\nabla \cdot \mathbf{B} = 0 \tag{2.24}$$

$$\nabla \times \mathbf{E} = -\frac{\partial \mathbf{B}}{\partial t} \tag{2.25}$$

$$\nabla \times \mathbf{B} = \mu_0 \epsilon_0 \frac{\partial \mathbf{E}}{\partial t} \tag{2.26}$$

Taking the curl of the Eqs. (2.25), (2.26), and using the curl of the curl identity we obtain

$$\mu_0\epsilon_0\frac{\partial^2\mathbf{E}}{\partial t^2} - \nabla^2\mathbf{E} = 0 \tag{2.27}$$

$$\mu_0\epsilon_0\frac{\partial^2\mathbf{B}}{\partial t^2} - \nabla^2\mathbf{B} = 0 \tag{2.28}$$

These equations have the form of the standard wave equation, that supports plane wave solutions $\mathbf{E} = E_0 e^{(\mathbf{k}\cdot\mathbf{r}-\omega t)}$, with dispersion relation $\omega = c|\mathbf{k}|$ [17].

Since $\nabla \cdot \mathbf{B} = 0$, the electromagnetic field can be written as the curl of a vector potential.

$$\mathbf{B} = \nabla \times \mathbf{A} \tag{2.29}$$

From this vector potential and Faraday's law, a scalar potential can be defined as follows[19]:

$$\nabla \times \mathbf{E} + \frac{\partial}{\partial t}(\nabla \times \mathbf{A}) = 0 \rightarrow -\nabla\phi = \mathbf{E} + \frac{\partial \mathbf{A}}{\partial t} \tag{2.30}$$

$$\mathbf{E} = -\nabla\phi - \frac{\partial \mathbf{A}}{\partial t} \tag{2.31}$$

Thus, we now have two expressions that give us the shape of the fields $\mathbf{E}$ and $\mathbf{B}$ as a function of two potentials $\mathbf{A}$ and ϕ. However, these potentials offer a certain freedom in their selection, which gives them an important characteristic: a caliber symmetry [18].

2.3.1 Gauge Transformation

The vector potential is not uniquely determined under preceding hypothesis, although invariant physically relevant quantity $\mathbf{B}$ is obviously invariant under a gauge transformation of the vector potential:

$$A \rightarrow A' = A + \nabla\chi \tag{2.32}$$

χ migth be an arbitrary scalar funtion, provided that the conditions is satisfied in every case $\nabla \times (\nabla\chi) = 0$ [18].

To simultaneously integrate the scalar potential ϕ, the electric field $\mathbf{E}$ must also be invariant under this change of magnitude. By proposing a general modification of the form $\phi' = \phi + \beta$ and substituting the new transformed vector potential into the field equation, we arrive at the condition that $\nabla\left(\beta + \frac{\partial\chi}{\partial t}\right) = 0$. This implies that the term in parentheses is independent of position and can only depend on time, defining a function $k(t)$. Finally, by absorbing this purely temporal dependence through a suitable redefinition of the scalar function χ, the transformation rule required for the scalar potential is uniquely deduced:

$$\phi' = \phi - \frac{\partial\chi}{\partial t} \tag{2.33}$$

In this way, by simultaneously applying both transformations, the real electromagnetic fields **E** and **B** are preserved intact [17].

2.3.2 Coulumb Gauge

The Coulomb gauge, also known as the transverse gauge, is defined by a mathematical restriction on the potential vector **A** [20, 21] :

$$\nabla \cdot \mathbf{A} = 0 \tag{2.34}$$

This condition is based on Helmholtz's descomposition theorem, which states that any smooth vector field can be separated into a longitudinal component (without curl) and a transverse component (without divergencen) [22], by imposing Eq.(2.34), the longitudinal vector component is completely eliminated, leaving just two transverse degrees of freedom corresponding to the two physical poralization states of the photon. So, under this condition, Maxwell's equiation behave as follows; the scalar potential datifies the Poisson equation $\nabla^2\phi = -\rho/\epsilon_0$, but, since we work in vacuum where $\rho = 0$ this reduces to $\nabla^2\phi = 0$, whose only Physically solution is $\phi = 0$ [23]. Therefore, all of physical information is encoded entirely in **A**, which satifies the wave equation:

$$\nabla^2 A - \frac{1}{c^2}\frac{\partial^2 A}{\partial t^2} = 0 \tag{2.35}$$

This gauge is particularly convenient for canonical quantization of the electromagnetic field, since the non-physical degrees of freedom are eliminated before quantization, thus simplifying the calculations, and the two remaining modes correspond exactly to the two polarization states of the physical photon [24].

2.3.3 Normal modes and Fourier decomposition

To discretize the field modes and significantly simplify the calculation, the electromagnetic field is confined in a cubic box of side L and volume $V = L^3$ Fig. (2.2). Assuming a source-free cavity without currents, charges, or dielectric media, we impose periodic boundary conditions ar the box's sides. This periodicity implies that only full wavelengths fit into the box , for a three-dimensional space [17, 25], the boundary conditions are:

$$\begin{aligned}
\mathbf{A}(L, y, z, t) &= \mathbf{A}(0, y, z, t) \\
\mathbf{A}(x, L, z, t) &= \mathbf{A}(x, 0, z, t) \\
\mathbf{A}(x, y, L, t) &= \mathbf{A}(x, y, 0, t)
\end{aligned}$$

Since the electromagnetic field in a vacuum is homogeneous, translationally invariant, and local, the natural basis for its expansion is a set of plane wave modes, which leads us to the following ansantz:

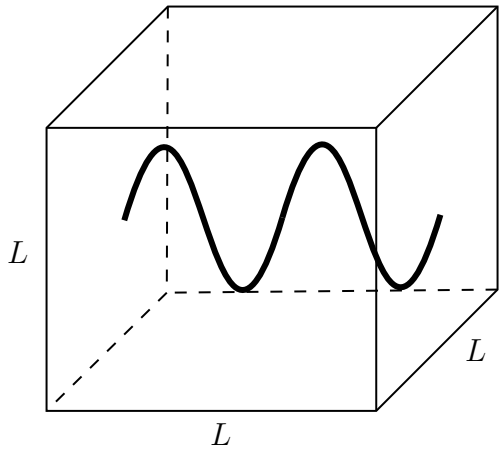


Figure 2.2: . The electromagnetic field is confined to a box

$$\mathbf{A}(x,y,z,t) = \mathbf{A}(x,y,z)e^{i\omega t} \tag{2.36}$$

Replacing this into the wave equation Eq. (2.35)

$$\nabla^2(\mathbf{A}(x,y,z)e^{i\omega t}) - \frac{1}{c^2}\frac{\partial^2}{\partial t^2}(\mathbf{A}(x,y,z)e^{i\omega t}) = 0$$
$$\Big(\Delta + \frac{\omega^2}{c^2}\Big)\mathbf{A}(x,y,z) = 0 \tag{2.37}$$

The Eq. (2.37), is known as The Hemlholtz Equation. A normal solution is given by:

$$\mathbf{A}_{\mathbf{k}\sigma} = N_{\mathbf{k}}\boldsymbol{\varepsilon}_{\mathbf{k}\sigma}e^{i\mathbf{k}\cdot\mathbf{x}} \qquad \text{with} \qquad (\sigma = 1,2) \tag{2.38}$$

The normal solution $\mathbf{A}_{\mathbf{k}\sigma}$ satisfies the Helmholtz equation provided the dispersion relation holds [17]:

$$\mathbf{k}^2 = \mathbf{k}_x^2 + \mathbf{k}_y^2 + \mathbf{k}_z^2 = \frac{\omega_k^2}{c^2} \tag{2.39}$$

or equivalently:

$$\omega_k^2 = c^2\mathbf{k} \tag{2.40}$$

The vectors $\varepsilon_{\mathbf{k}\sigma}$ are the polarization vectors associated with the wave vector $\mathbf{k}$, and the index $\sigma = 1,2$ labels are the two field-independent polarization states. Since we are working into Coulomb gauge, substituting the normal solution into this condition yields [17]:

$$\boldsymbol{\varepsilon}\cdot\mathbf{k} = 0 \tag{2.41}$$

This means that the polarization vectors are strictly perpendicular to the propagation direction $\mathbf{k}$,the two polarization vectors represent the two independent transverse degrees of freedom of the photon, reflecting their purely transverse nature to the propagation of electromagnetic waves in a vacuum [26]. For each wave vector $\mathbf{k}$, two linearly independent polarization vectors $\varepsilon_{\mathbf{k}1}$ and $\varepsilon_{\mathbf{k}2}$, both contained in the plane perpendicular to $\mathbf{k}$, can be chosen that satisfy the orthonormality condition [17][7]:

$$\boldsymbol{\varepsilon}_{\mathbf{k}\sigma} \cdot \boldsymbol{\varepsilon}_{\mathbf{k}\sigma'} = \delta_{\sigma\sigma'} \tag{2.42}$$

Along with $\hat{\mathbf{k}} = \mathbf{k}/|\mathbf{k}|$, these two vectors form an orthonormal triad with positive orientation:

$$\boldsymbol{\varepsilon}_{\mathbf{k}1} \times \boldsymbol{\varepsilon}_{\mathbf{k}2} = \hat{\mathbf{k}} \tag{2.43}$$

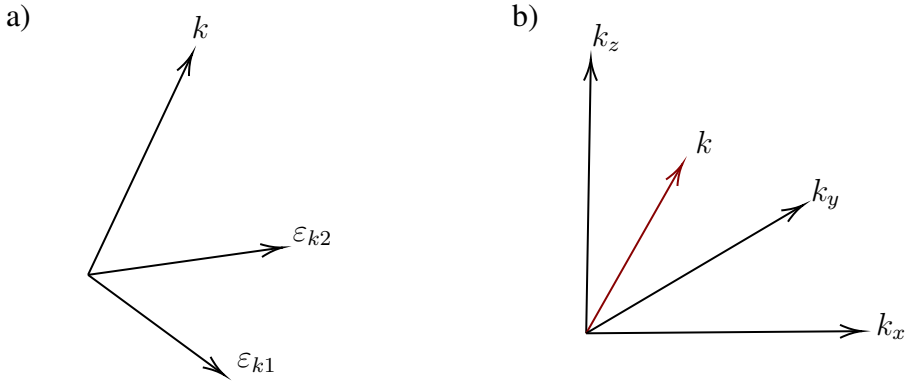


Figure 2.3: Polarization vectors and illustration of k-space

In order to fulfill the boundary conditions, the wave vector has to take on the form

$$\mathbf{k} = (k_x, k_y, k_z) = \frac{2\pi}{L}(n_1, n_2, n_3), \qquad n_1, n_2, n_3 \in \mathbb{Z} \tag{2.44}$$

The most general solution for the field $\mathbf{A}$ is now a superposition of all the normal modes. Due to the spatial part of each normal mode is a complex exponential with forms $e^{i\mathbf{k}\cdot\mathbf{x}}$, this superposition is equal to a Fourier series:

$$\mathbf{A}(\mathbf{x}, t) = \sum_{\substack{\mathbf{k} \\ k_z>0}} \sum_{\sigma=1,2} [a_{\boldsymbol{k}\sigma}(t)\mathbf{A}_{\boldsymbol{k}\sigma}(x) + a^*_{\boldsymbol{k}\sigma}(t)\mathbf{A}^*_{\boldsymbol{k}\sigma}(x)] \tag{2.45}$$

replacing Eq. (2.38) in Eq. (2.45)

$$\mathbf{A}(\mathbf{x}, t) = \sum_{\substack{\mathbf{k} \\ k_z>0}} \sum_{\sigma=1,2} N_{\mathbf{k}} \boldsymbol{\varepsilon}_{\mathbf{k}\sigma} \left(a_{\mathbf{k}\sigma}(t)\, e^{i\mathbf{k}\cdot\mathbf{x}} + a^*_{\mathbf{k}\sigma}(t)\, e^{-i\mathbf{k}\cdot\mathbf{x}} \right) \tag{2.46}$$

Since the field $\mathbf{A}$ must be real and measurable, we must sum the complex conjugate of each term, thus ensuring that the sum results in a real number. Because the terms

$e^{i\mathbf{k}\cdot\mathbf{x}}$ and $e^{-i\mathbf{k}\cdot\mathbf{x}}$ in the expansion are related by complex conjugation, the modes $\mathbf{k}$ and $-\mathbf{k}$ describe the same physical degree of freedom and should not be counted twice. To avoid this redundancy, the sum is restricted to $k_z > 0$, ensuring that for each pair $(\mathbf{k}, -\mathbf{k})$ only one representative enters the sum [17].

Now, the coefficients of the Fourier series are promoted to operators, where $a_{\boldsymbol{k}\sigma}$ will be the annihilation operator and $a^*_{\boldsymbol{k}\sigma}$ will be the creation operator. Then, the results of the expansion Eq. (2.45) are substituted into the wave equation Eq. (2.35):

$$\left(\nabla^2 - \frac{1}{c^2}\frac{\partial^2}{\partial t^2}\right) \sum_{\substack{\mathbf{k},\sigma \\ k_z>0}} N_{\mathbf{k}}\, \boldsymbol{\varepsilon}_{\mathbf{k}\sigma} \left(a_{\mathbf{k}\sigma}(t)\, e^{i\mathbf{k}\cdot\mathbf{x}} + a^*_{\mathbf{k}\sigma}(t)\, e^{-i\mathbf{k}\cdot\mathbf{x}}\right) = 0 \tag{2.47}$$

$$\sum_{\substack{\mathbf{k},\sigma \\ k_z>0}} N_{\mathbf{k}}\, \boldsymbol{\varepsilon}_{\mathbf{k}\sigma} \left[\nabla^2 \left(a_{\mathbf{k}\sigma}(t)\, e^{i\mathbf{k}\cdot\mathbf{x}}\right) + \nabla^2 \left(a^*_{\mathbf{k}\sigma}(t)\, e^{-i\mathbf{k}\cdot\mathbf{x}}\right) - \frac{1}{c^2}\frac{\partial^2}{\partial t^2}\left(a_{\mathbf{k}\sigma}(t)\, e^{i\mathbf{k}\cdot\mathbf{x}}\right) - \frac{1}{c^2}\frac{\partial^2}{\partial t^2}\left(a^\dagger_{\mathbf{k}\sigma}(t)\, e^{-i\mathbf{k}\cdot\mathbf{x}}\right)\right] = 0$$

whose development is:

$$\begin{aligned}
\nabla^2 \left(a_{\mathbf{k}\sigma}(t)\, e^{i\mathbf{k}\cdot\mathbf{x}}\right) &= -k^2\, a_{\mathbf{k}\sigma}(t)\, e^{i\mathbf{k}\cdot\mathbf{x}} \\
\nabla^2 \left(a^*_{\mathbf{k}\sigma}(t)\, e^{-i\mathbf{k}\cdot\mathbf{x}}\right) &= -k^2\, a^*_{\mathbf{k}\sigma}(t)\, e^{-i\mathbf{k}\cdot\mathbf{x}} \\
\frac{\partial^2}{\partial t^2}\left(a_{\mathbf{k}\sigma}(t)\, e^{i\mathbf{k}\cdot\mathbf{x}}\right) &= \frac{d^2 a_{\mathbf{k}\sigma}}{dt^2}\, e^{i\mathbf{k}\cdot\mathbf{x}} \\
\frac{\partial^2}{\partial t^2}\left(a^*_{\mathbf{k}\sigma}(t)\, e^{-i\mathbf{k}\cdot\mathbf{x}}\right) &= \frac{d^2 a^*_{\mathbf{k}\sigma}}{dt^2}\, e^{-i\mathbf{k}\cdot\mathbf{x}}
\end{aligned}$$

then

$$\left(-\mathbf{k}^2 a_{\mathbf{k}\sigma} - \frac{1}{c^2}\frac{d^2}{dt^2} a_{\mathbf{k}\sigma}\right) e^{i\mathbf{k}\cdot\mathbf{x}} \tag{2.48}$$

Consequently, the unique requirement for the sum to equal zero is that the differential equation must vanish:

$$\frac{d^2}{dt^2} a_{\mathbf{k}\sigma} + \mathbf{k}^2 c^2 a_{\mathbf{k}\sigma} = 0 \qquad \text{or} \qquad \frac{d^2}{dt^2} a_{\mathbf{k}\sigma} + \omega^2_{\mathbf{k}} a_{\mathbf{k}\sigma} = 0 \tag{2.49}$$

This yields the equation for each mode, which is the harmonic oscillator equation, Its general solution is a linear combination of $e^{-i\omega_{\mathbf{k}} t}$ and $e^{i\omega_{\mathbf{k}} t}$

$$a_{\mathbf{k}\sigma}(t) = a^{(1)}_{\mathbf{k}\sigma}(0) e^{-i\omega_{\mathbf{k}} t} + a^{(2)}_{\mathbf{k}\sigma}(0) e^{i\omega_{\mathbf{k}} t} \tag{2.50}$$

Replacing Eq. (2.50) into the original expansion Eq. (2.46)

$$\mathbf{A}(x,t) = \sum_{\substack{\mathbf{k},\sigma \\ k_z>0}} N_{\mathbf{k}} \boldsymbol{\varepsilon}_{\mathbf{k}\sigma} \left[\left(a^{(1)}_{\mathbf{k}\sigma}(0) e^{-i\omega_{\mathbf{k}} t} + a^{(2)}_{\mathbf{k}\sigma}(0) e^{i\omega_{\mathbf{k}} t} \right) e^{i\mathbf{k}\cdot\mathbf{x}} + \left(a^{(1)*}_{\mathbf{k}\sigma}(0) e^{-i\omega_{\mathbf{k}} t} + a^{(2)*}_{\mathbf{k}\sigma}(0) e^{i\omega_{\mathbf{k}} t} \right) e^{-i\mathbf{k}\cdot\mathbf{x}} \right] \tag{2.51}$$

We regroup the terms according to the spatiotemporal phase

$$\begin{aligned} a^{(1)}_{\mathbf{k}\sigma}(0) e^{-i\omega_{\mathbf{k}} t}\, e^{i\mathbf{k}\cdot\mathbf{x}} &= a^{(1)} e^{i(\mathbf{k}\cdot\mathbf{x}-\omega_{\mathbf{k}} t)} \\ a^{(1)*}_{\mathbf{k}\sigma}(0) e^{i\omega_{\mathbf{k}} t}\, e^{-i\mathbf{k}\cdot\mathbf{x}} &= a^{(1)*r} e^{-i(\mathbf{k}\cdot\mathbf{x}-\omega_{\mathbf{k}} t)} \\ a^{(2)}_{\mathbf{k}\sigma}(0) e^{i\omega_{\mathbf{k}} t}\, e^{i\mathbf{k}\cdot\mathbf{x}} &= a^{(2)} e^{i(\mathbf{k}\cdot\mathbf{x}+\omega_{\mathbf{k}} t)} \\ a^{(2)*}_{\mathbf{k}\sigma}(0) e^{-i\omega_{\mathbf{k}} t}\, e^{-i\mathbf{k}\cdot\mathbf{x}} &= a^{(2)*} e^{-i(\mathbf{k}\cdot\mathbf{x}+\omega_{\mathbf{k}} t)} \end{aligned}$$

Thus we obtain the expression

$$\begin{aligned} \mathbf{A}(x,t) = \sum_{\mathbf{k},\sigma} N_{\mathbf{k}} \boldsymbol{\varepsilon}_{\mathbf{k}\sigma} \Big[& a^{(1)}_{\mathbf{k}\sigma}(0) e^{i(\mathbf{k}\cdot\mathbf{x}-\omega_{\mathbf{k}} t)} + a^{(1)*}_{\mathbf{k}\sigma}(0) e^{-i(\mathbf{k}\cdot\mathbf{x}-\omega_{\mathbf{k}} t)} + a^{(2)}_{\mathbf{k}\sigma}(0) e^{i(\mathbf{k}\cdot\mathbf{x}+\omega_{\mathbf{k}} t)} \\ & + a^{(2)*}_{\mathbf{k}\sigma}(0) e^{-i(\mathbf{k}\cdot\mathbf{x}+\omega_{\mathbf{k}} t)} \Big] \end{aligned} \tag{2.52}$$

Orientations of Vector Spaces

Let $\mathbf{V}$ be a real vector space of dimention $n \geq 1$ two ordered bases $(E_1, ..., E_n)$ and $(\tilde{E}_1, ..., \tilde{E}_n)$ are said to hace same orientation if the change of bases matrix B^j_i, define by

$$E_i = B^j_i \tilde{E}_j$$

has a positive determinant $(det(B^j_i) > 0)$.

This relation divides the set of all ordered bases of V into two classes. An orientation of the vector space consists of choosing one of these two classes as the positive orientation; bases belonging to that class are called positively oriented, while those of the other class are considered negatively oriented [27].

Given that the restriction $\mathbf{k} > 0$ is awkward, the free constants $a^{(1)}_{\mathbf{k}\sigma}(0)$ and $a^{(2)}_{\mathbf{k}\sigma}(0)$ are redefined as:

$$a^{(1)}_{\mathbf{k}\sigma}(0) = a_{\mathbf{k}\sigma}(0) \qquad a^{(2)}_{\mathbf{k}\sigma}(0) = -(-1)^{\sigma} a^{*}_{\mathbf{k}\sigma}(0) \qquad \text{for } \mathbf{k}_z > 0 \tag{2.53}$$

Then Eq. (2.52) transforms into

$$\begin{aligned} \mathbf{A}(x,t) = \sum_{\substack{\mathbf{k},\sigma \\ k_z>0}} N_{\mathbf{k}} \boldsymbol{\varepsilon}_{\mathbf{k}\sigma} \Big[& a_{\mathbf{k}\sigma}(0) e^{i(\mathbf{k}\cdot\mathbf{x}-\omega_{\mathbf{k}} t)} + a^{*}_{\mathbf{k}\sigma}(0) e^{-i(\mathbf{k}\cdot\mathbf{x}-\omega_{\mathbf{k}} t)} \\ & - (-1)^{\sigma} \left(a^{*}_{-\mathbf{k}\sigma}(0) e^{i(\mathbf{k}\cdot\mathbf{x}+\omega_{\mathbf{k}} t)} + a_{-\mathbf{k}\sigma}(0) e^{-i(\mathbf{k}\cdot\mathbf{x}+\omega_{\mathbf{k}} t)} \right) \Big] \end{aligned} \tag{2.54}$$

This redefinition is consistent with the transformation of the polarization vectors under the inversion of $\mathbf{k}$, mamely

$$\boldsymbol{\varepsilon}_{-\mathbf{k}\sigma} = -(-1)^{\sigma}\boldsymbol{\varepsilon}_{\mathbf{k}\sigma} \tag{2.55}$$

$$\begin{aligned}\mathbf{A}(x,t) = &\sum_{\substack{\mathbf{k},\sigma \\ k_z>0}} N_{\mathbf{k}}\boldsymbol{\varepsilon}_{\mathbf{k}\sigma}\left[a_{\mathbf{k}\sigma}(0)e^{i(\mathbf{k}\cdot\mathbf{x}-\omega_{\mathbf{k}}t)} + a^{*}_{\mathbf{k}\sigma}(0)e^{-i(\mathbf{k}\cdot\mathbf{x}-\omega_{\mathbf{k}}t)}\right] \\ &+ \sum_{\substack{\mathbf{k},\sigma \\ k_z>0}} N_{\mathbf{k}}\boldsymbol{\varepsilon}_{-\mathbf{k}\sigma}\left[a^{*}_{-\mathbf{k}\sigma}(0)e^{i(\mathbf{k}\cdot\mathbf{x}+\omega_{\mathbf{k}}t)} + a_{-\mathbf{k}\sigma}(0)e^{-i(\mathbf{k}\cdot\mathbf{x}+\omega_{\mathbf{k}}t)}\right]\end{aligned}$$

Reindexing the terms of the second summation ($\mathbf{k} \to -\mathbf{k}$)

$$\begin{aligned}a^{*}_{-\mathbf{k}\sigma}(0)e^{i(\mathbf{k}\cdot\mathbf{x}+\omega_{\mathbf{k}}t)} &\to a^{*}_{\mathbf{k}\sigma}(0)e^{i((-\mathbf{k})\cdot\mathbf{x}+\omega_{\mathbf{k}}t)} \\ &= a^{*}_{\mathbf{k}\sigma}(0)e^{i(-\mathbf{k}\cdot\mathbf{x}+\omega_{\mathbf{k}}t)} \\ &= a^{*}_{\mathbf{k}\sigma}(0)e^{-i(\mathbf{k}\cdot\mathbf{x}-\omega_{\mathbf{k}}t)}\end{aligned}$$

Note: $\omega_{\mathbf{k}} = c|-\mathbf{k}| = c|\mathbf{k}| = \omega_{\mathbf{k}}$the frequency does not change because it only depends on the module.

$$\begin{aligned}a_{-\mathbf{k}\sigma}(0)e^{i(\mathbf{k}\cdot\mathbf{x}+\omega_{\mathbf{k}}t)} &\to a_{\mathbf{k}\sigma}(0)e^{-i((-\mathbf{k})\cdot\mathbf{x}+\omega_{\mathbf{k}}t)} \\ &= a_{\mathbf{k}\sigma}(0)e^{-i(-\mathbf{k}\cdot\mathbf{x}+\omega_{\mathbf{k}}t)} \\ &= a_{\mathbf{k}\sigma}(0)e^{i(\mathbf{k}\cdot\mathbf{x}-\omega_{\mathbf{k}}t)}\end{aligned}$$

Base Orientation

In this case, the positive orientation is conventionally adopted as that of the canonical basis (e_x, e_y, e_z) known as the right-hand basis $(e_x \times e_y = e_z)$. Equivalently, an orthonormal basis (e_1, e_2, e_3) is right-oriented if it satisfies $(e_1 \times e_2 = e_3)$.

Since this segment spans $-\mathbf{k}$, then the sum is over $\mathbf{k}_z < 0$

$$\sum_{\substack{\mathbf{k},\sigma \\ k_z<0}} N_{\mathbf{k}}\boldsymbol{\varepsilon}_{\mathbf{k}\sigma}\left[a^{*}_{\mathbf{k}\sigma}(0)e^{i(\mathbf{k}\cdot\mathbf{x}+\omega_{\mathbf{k}}t)} + a_{\mathbf{k}\sigma}(0)e^{-i(\mathbf{k}\cdot\mathbf{x}+\omega_{\mathbf{k}}t)}\right] \tag{2.56}$$

Which has exactly the formula of the first part of the expansion. Now we do

$$\begin{aligned}\mathbf{A}(x,t) = &\sum_{\substack{\mathbf{k},\sigma \\ k_z>0}} N_{\mathbf{k}}\boldsymbol{\varepsilon}_{\mathbf{k}\sigma}\left[a_{\mathbf{k}\sigma}(0)e^{i(\mathbf{k}\cdot\mathbf{x}-\omega_{\mathbf{k}}t)} + a^{*}_{\mathbf{k}\sigma}(0)e^{-i(\mathbf{k}\cdot\mathbf{x}-\omega_{\mathbf{k}}t)}\right] \\ &+ \sum_{\substack{\mathbf{k},\sigma \\ k_z<0}} N_{\mathbf{k}}\boldsymbol{\varepsilon}_{\mathbf{k}\sigma}\left[a_{\mathbf{k}\sigma}(0)e^{i(\mathbf{k}\cdot\mathbf{x}+\omega_{\mathbf{k}}t)} + a^{*}_{\mathbf{k}\sigma}(0)e^{-i(\mathbf{k}\cdot\mathbf{x}+\omega_{\mathbf{k}}t)}\right]\end{aligned} \tag{2.57}$$

Both summations have the same form and their ranks are disjoint and complementary.

$$\{\mathbf{k}_z > 0\} \cup \{\mathbf{k}_z < 0\} = \{\text{all the } \mathbf{k} \text{ except } \mathbf{k} = 0\}$$

They merge into a single sum:

$$\mathbf{A}(x,t) = \sum_{\mathbf{k},\sigma} N_{\mathbf{k}} \boldsymbol{\varepsilon}_{\mathbf{k}\sigma} \left[a_{\mathbf{k}\sigma}(0) e^{i(\mathbf{k}\cdot\mathbf{x} - \omega_{\mathbf{k}} t)} + a^*_{\mathbf{k}\sigma}(0) e^{-i(\mathbf{k}\cdot\mathbf{x} - \omega_{\mathbf{k}} t)} \right] \tag{2.58}$$

Defining $a_{\mathbf{k}\sigma}(t) = a_{\mathbf{k}\sigma}(0) e^{\omega_{\mathbf{k}} t}$, the expansion Eq. (2.58) is compactly described as:

$$\mathbf{A}(x,t) = \sum_{\mathbf{k},\sigma} N_{\mathbf{k}} \boldsymbol{\varepsilon}_{\mathbf{k}\sigma} \left[a_{\mathbf{k}\sigma}(0) e^{i\mathbf{k}\cdot\mathbf{x}} + a^*_{\mathbf{k}\sigma}(0) e^{-i\mathbf{k}\cdot\mathbf{x}} \right] \tag{2.59}$$

Which is consistent with Eq. (2.49). From this relation is follows that [17]:

$$\frac{da_{\mathbf{k}\sigma}(t)}{dt} = -i\omega_{\mathbf{k}} a_{\mathbf{k}\sigma}(t) \tag{2.60}$$

2.3.4 Energy of the Electromagnetic Field

To construct the Hamiltonian of the electromagnetic field in a box of volume L^3, we start from the classical energy density expressed in terms of the vector potential in the transverse regime ($\boldsymbol{\nabla} \cdot \mathbf{A} = 0$).The energy of the field is given by [25]:

$$H = \frac{1}{8\pi} \int_{L^3} d^3x (\mathbf{E}^2 + \mathbf{B}^2) \tag{2.61}$$

$$H = \frac{1}{8\pi} \int_{L^3} d^3 \left[\frac{1}{c^2} \frac{\partial \mathbf{A}}{\partial t} \cdot \frac{\partial \mathbf{A}^*}{\partial t} + (\nabla \times \mathbf{A}) \cdot (\nabla \times \mathbf{A}^*) \right] \tag{2.62}$$

Now we insert the Fourier expansion

$$\frac{\partial \mathbf{A}}{\partial t} = \sum_{\mathbf{k},\sigma} N_{\mathbf{k}} \boldsymbol{\varepsilon}_{\mathbf{k}\sigma} \left[(-i\omega_{\mathbf{k}}) a_{\mathbf{k}\sigma} e^{i\mathbf{k}\cdot\mathbf{x}} + (i\omega_{\mathbf{k}}) a^*_{\mathbf{k}\sigma} e^{-i\mathbf{k}\cdot\mathbf{x}} \right]$$

factoring $i\mathbf{k}$

$$\frac{\partial \mathbf{A}}{\partial t} = -i \sum_{\mathbf{k},\sigma} \omega_k N_k \boldsymbol{\varepsilon}_{k\sigma} \left[a_{k\sigma} e^{i\mathbf{k}\cdot\mathbf{r}} - a^*_{k\sigma} e^{-i\mathbf{k}\cdot\mathbf{r}} \right] \tag{2.63}$$

Taking the complex conjugate of the previous expression (remembering that $i \to -i$ and the operators are conjugated):

$$\frac{\partial \mathbf{A}^*}{\partial t} = i \sum_{\mathbf{k}',\sigma'} \omega_{k'} N^*_{k'} \boldsymbol{\varepsilon}^*_{k'\sigma'} \left[a^*_{k'\sigma'} e^{-i\mathbf{k}'\cdot\mathbf{r}} - a_{k'\sigma'} e^{i\mathbf{k}'\cdot\mathbf{r}} \right]$$

Inverting the sign inside the bracket and removing a negative sign:

$$\frac{\partial \mathbf{A}^*}{\partial t} = -i \sum_{\mathbf{k}',\sigma'} \omega_{k'} N^*_{k'} \boldsymbol{\varepsilon}^*_{k'\sigma'} \left[a_{k'\sigma'} e^{i\mathbf{k}'\cdot\mathbf{r}} - a^*_{k'\sigma'} e^{-i\mathbf{k}'\cdot\mathbf{r}} \right] \tag{2.64}$$

Now we can make the dot product

$$\frac{\partial \mathbf{A}}{\partial t}\cdot\frac{\partial \mathbf{A}^*}{\partial t} = -\sum_{\mathbf{k},\sigma}\sum_{\mathbf{k}',\sigma'}\omega_k\omega_{k'}N_kN^*_{k'}(\boldsymbol{\varepsilon}_{k\sigma}\cdot\boldsymbol{\varepsilon}^*_{k'\sigma'})\left(a_{k\sigma}e^{i\mathbf{k}\cdot\mathbf{r}} - a^*_{k\sigma}e^{-i\mathbf{k}\cdot\mathbf{r}}\right)\left(a_{k'\sigma'}e^{i\mathbf{k}'\cdot\mathbf{r}} - a^*_{k'\sigma'}e^{-i\mathbf{k}'\cdot\mathbf{r}}\right)$$

In the integral $\int d^3x \frac{1}{8\pi c^2}\frac{\partial \mathbf{A}}{\partial t}\cdot\frac{\partial \mathbf{A}^*}{\partial t}$, taking the constants and sums out of the integral:

$$= -\sum_{\mathbf{k},\sigma}\sum_{\mathbf{k}',\sigma'}\frac{\omega_k\omega_{k'}}{8\pi c^2}N_kN^*_{k'}(\boldsymbol{\varepsilon}_{k\sigma}\cdot\boldsymbol{\varepsilon}^*_{k'\sigma'})\int d^3x\left(a_{k\sigma}e^{i\mathbf{k}\cdot\mathbf{r}} - a^*_{k\sigma}e^{-i\mathbf{k}\cdot\mathbf{r}}\right)\left(a_{k'\sigma'}e^{i\mathbf{k}'\cdot\mathbf{r}} - a^*_{k'\sigma'}e^{-i\mathbf{k}'\cdot\mathbf{r}}\right)$$

we can exploit the orthogonality relations [17]

$$\int_{L^3} d^3x\, e^{i\mathbf{k}\cdot\mathbf{r}}e^{-i\mathbf{k}'\cdot\mathbf{r}} = L^3\delta_{\mathbf{k}\mathbf{k}'} \tag{2.65}$$

and

$$\boldsymbol{\varepsilon}_{\mathbf{k}\sigma}\cdot\boldsymbol{\varepsilon}_{\mathbf{k}\sigma'} = \delta_{\sigma\sigma'}$$

$$\boldsymbol{\varepsilon}_{\mathbf{k}\sigma}\cdot\boldsymbol{\varepsilon}_{-\mathbf{k}\sigma'} = -(-1)^{\sigma}\delta_{\sigma\sigma'}$$

Therefore

$$\int_{L^3} d^3x\,\frac{1}{8\pi c^2}\frac{\partial \mathbf{A}}{\partial t}\cdot\frac{\partial \mathbf{A}^*}{\partial t} = \sum_{\mathbf{k},\sigma}\frac{\omega_k^2}{8\pi c^2}N_k^2L^3\left[\{a_{\mathbf{k}\sigma}a^*_{\mathbf{k}\sigma} + a^*_{\mathbf{k}\sigma}a_{\mathbf{k}\sigma}\} + (-1)^{\sigma}\{a_{\mathbf{k}\sigma}a_{-\mathbf{k}\sigma} + a^*_{\mathbf{k}\sigma}a^*_{-\mathbf{k}\sigma}\}\right] \tag{2.66}$$

Now we will develop the rotational part; for this we use the identity:

$$\boldsymbol{\nabla}\times\left(\mathbf{V}e^{i\mathbf{k}\cdot\mathbf{r}}\right) = i\mathbf{k}\times\mathbf{V}e^{i\mathbf{k}\cdot\mathbf{r}} \tag{2.67}$$

Thus,using Eq. (2.67) the curl of the vector potential field can be written as:

$$\boldsymbol{\nabla}\times\mathbf{A} = \sum_{\mathbf{k},\sigma}N_k\left[a_{\mathbf{k}\sigma}(i\mathbf{k}\times\boldsymbol{\varepsilon}_{\mathbf{k}\sigma})e^{i\mathbf{k}\cdot\mathbf{r}} + a^*_{\mathbf{k}\sigma}(-i\mathbf{k}\times\boldsymbol{\varepsilon}_{\mathbf{k}\sigma})e^{-i\mathbf{k}\cdot\mathbf{r}}\right]$$

Factoring i

$$\boldsymbol{\nabla}\times\mathbf{A} = i\sum_{\mathbf{k},\sigma}N_k(\mathbf{k}\times\boldsymbol{\varepsilon}_{\mathbf{k}\sigma})\left[a_{\mathbf{k}\sigma}e^{i\mathbf{k}\cdot\mathbf{r}} - a^*_{\mathbf{k}\sigma}e^{-i\mathbf{k}\cdot\mathbf{r}}\right]$$

So, the product of both curls

$$\begin{aligned}(\boldsymbol{\nabla}\times\mathbf{A})\cdot(\boldsymbol{\nabla}\times\mathbf{A}^*) = (i)(-i)\sum_{\mathbf{k},\sigma}\sum_{\mathbf{k}',\sigma'}N_kN_{k'}\left[(\mathbf{k}\times\boldsymbol{\varepsilon}_{\mathbf{k}\sigma})\cdot(\mathbf{k}'\times\boldsymbol{\varepsilon}_{\mathbf{k}'\sigma'})\right]\\ \cdot\left(a_{\mathbf{k}\sigma}e^{i\mathbf{k}\cdot\mathbf{r}} - a^*_{\mathbf{k}\sigma}e^{-i\mathbf{k}\cdot\mathbf{r}}\right)\cdot\left(a_{\mathbf{k}'\sigma'}e^{i\mathbf{k}'\cdot\mathbf{r}} - a^*_{\mathbf{k}'\sigma'}e^{-i\mathbf{k}'\cdot\mathbf{r}}\right)\end{aligned} \tag{2.68}$$

When evaluating spatial deltas, we analyze vector products under the same two conditions:

1. With $\mathbf{k}' = \mathbf{k}$ the vector product is $(\mathbf{k} \times \boldsymbol{\varepsilon}_{\mathbf{k}\sigma}) \cdot (\mathbf{k} \times \boldsymbol{\varepsilon}_{\mathbf{k}\sigma'})$. Using the Lagrangian identity:
$$(\mathbf{A} \times \mathbf{B}) \cdot (\mathbf{C} \times \mathbf{D}) = (\mathbf{A} \cdot \mathbf{C})(\mathbf{B} \cdot \mathbf{D}) - (\mathbf{A} \cdot \mathbf{D})(\mathbf{B} \cdot \mathbf{C})$$
We identified that:
$$(\mathbf{k} \times \boldsymbol{\varepsilon}_{\mathbf{k}\sigma}) \cdot (\mathbf{k} \times \boldsymbol{\varepsilon}_{\mathbf{k}\sigma'}) = (\mathbf{k} \cdot \mathbf{k})(\boldsymbol{\varepsilon}_{\mathbf{k}\sigma} \cdot \boldsymbol{\varepsilon}_{\mathbf{k}\sigma'}) - (\mathbf{k} \cdot \boldsymbol{\varepsilon}_{\mathbf{k}\sigma'})(\boldsymbol{\varepsilon}_{\mathbf{k}\sigma} \cdot \mathbf{k}) \tag{2.69}$$
Since the field is purely transverse, Coulomb's condition requires that $\mathbf{k} \cdot \boldsymbol{\varepsilon}_{\mathbf{k}\sigma} = 0$. The second term vanishes completely, the expression reduces to: $k^2(\boldsymbol{\varepsilon}_{\mathbf{k}\sigma} \cdot \boldsymbol{\varepsilon}_{\mathbf{k}\sigma'}) = k^2\delta_{\sigma\sigma'}$ This gives us:
$$k^2 \left[a_{\mathbf{k}\sigma} a^*_{\mathbf{k}\sigma} + a^*_{\mathbf{k}\sigma} a_{\mathbf{k}\sigma}\right] \tag{2.70}$$
2. With $\mathbf{k}' = -\mathbf{k}$ the vector produc is $(\mathbf{k} \times \boldsymbol{\varepsilon}_{\mathbf{k}\sigma}) \cdot (-\mathbf{k} \times \boldsymbol{\varepsilon}_{-\mathbf{k}\sigma'})$. Replacing Eq. (2.55)
$$(\mathbf{k} \times \boldsymbol{\varepsilon}_{\mathbf{k}\sigma}) \cdot \left[-\mathbf{k} \times \left(-(-1)^{\sigma'} \boldsymbol{\varepsilon}_{\mathbf{k}\sigma'}\right)\right] = (-1)^{\sigma'} (\mathbf{k} \times \boldsymbol{\varepsilon}_{\mathbf{k}\sigma}) \cdot (\mathbf{k} \times \boldsymbol{\varepsilon}_{\mathbf{k}\sigma'}) = (-1)^{\sigma} k^2 \delta_{\sigma\sigma'} \tag{2.71}$$
Consequently
$$-(-1)^{\sigma} \left[a_{\mathbf{k}\sigma} a_{-\mathbf{k}\sigma} + a^*_{\mathbf{k}\sigma} a^*_{-\mathbf{k}\sigma}\right] \tag{2.72}$$

Remembering that for electromagnetic waves in a vacuum, $k^2 = \frac{\omega_k^2}{c^2}$ holds true:
$$= \sum_{\mathbf{k},\sigma} \frac{\omega_k^2}{8\pi c^2} N_k^2 L^3 \left[\left(a_{\mathbf{k}\sigma} a^*_{\mathbf{k}\sigma} + a^*_{\mathbf{k}\sigma} a_{\mathbf{k}\sigma}\right) - (-1)^{\sigma} \left(a_{\mathbf{k}\sigma} a_{-\mathbf{k}\sigma} + a^*_{\mathbf{k}\sigma} a^*_{-\mathbf{k}\sigma}\right)\right] \tag{2.73}$$

Adding both contributions Eq. (2.67) and Eq. (2.73) we obtain:
$$H = \sum_{\mathbf{k},\sigma} \frac{\omega_k^2}{4\pi c^2} N_k^2 L^3 \left(a_{\mathbf{k}\sigma} a^*_{\mathbf{k}\sigma} + a^*_{\mathbf{k}\sigma} a_{\mathbf{k}\sigma}\right) \tag{2.74}$$

Since this equation resembles a system of decoupled oscillators, you choose as the normalization constant[25]:
$$N_k = \sqrt{\frac{2\pi\hbar c^2}{L^3 \omega_k}} \quad \Longrightarrow \quad N_k^2 = \frac{2\pi\hbar c^2}{L^3 \omega_k} \tag{2.75}$$
Then, the energy of the electromagnetic field becomes equal to the sum of the energies corresponding to the "harmonic field oscillators"[25].
$$H = \frac{1}{2} \sum_{\mathbf{k},\sigma} \hbar\omega_k \left(a_{\mathbf{k}\sigma} a^*_{\mathbf{k}\sigma} + a^*_{\mathbf{k}\sigma} a_{\mathbf{k}\sigma}\right) \tag{2.76}$$

3

Casimir Effect

In 1948, Dutch physicists Hendrik B. G. Casimir and Dirk Polder, researchers at the Philips laboratories in Eindhoven, published a seminal paper incorporating retardation effects into the London-van der Waals force. This correction revealed behavior that differed from London's law at large distances. The theoretical adjustment was timely, as Verwey and Overbeek had experimentally demonstrated during the 1940s—using colloidal suspensions—that the long-range interaction decayed more rapidly than predicted [28]. After completing this work, Casimir traveled to Copenhagen to meet with his mentor, Niels Bohr. During one of their walks, Bohr suggested that the force could be calculated by evaluating differences in the zero-point energy of the electromagnetic field. Guided by this idea, Casimir completely reformulated the problem in terms of vacuum energy [29, 5]. Thus, Casimir predicted that two neutral, perfectly conducting parallel plates would attract each other with a force depending solely on the separation between them, Planck's constant, and the speed of light. This result, published in 1948, is known as the Casimir effect and constitutes one of the most direct manifestations of the existence of zero-point energy [29, 30]. Although theoretically elegant, experimentally verifying Casimir's prediction proved difficult. Maintaining perfect alignment between flat parallel plates separated by nanometric distances is practically impossible; small angular deviations severely distort the measurement. Consequently, as shown in Table 3.1, experimental efforts evolved from Sparnaay's pioneering initial attempts to modern sphere-plane geometries employing atomic force microscopy (AFM) and microelectromechanical systems (MEMS), which allowed for overcoming alignment issues and reducing experimental uncertainty to below 1%.

In general, the attractive or repulsive nature of the Casimir force depends on the geometry of the conducting surfaces and, even more importantly, on the imposed boundary conditions [39]. In this chapter, we will perform this calculation for three configurations: parallel flat plates, concentric cylinders, and concentric spherical shells.

3.1 Parallel plane plates

Let's consider a system consisting of two square plates of side length L inside a cubic cavity of volume L^3 whose walls are also perfectly conducting. One of our plates is fixed and coincides with one of the faces of the cavity, while the other is movable and

Table 3.1: Chronological summary of Casimir effect experiments: geometry, technique, and uncertainty.

Researchers	**Geometry**	**Technique / Device**	**Uncertainty**
M. J. Sparnaay (1958) [31]	Parallel plate-plate	Spring balance / Parallel-plate capacitance	$\sim 100\%$
van Blokland & Overbeek (1978) [32]	Plane-lens / Plane-plane	Torsion balance / Capacitive sensor	$\sim 25\% - 50\%$
S. K. Lamoreaux (1997) [33]	Sphere-plane	Torsion pendulum with piezoelectric actuator	$\sim 5\%$
U. Mohideen and A. Roy (1998) [34]	Sphere-plane	Atomic force microscope (AFM)	$\sim 1\%$
G. Bressi et al. (2002) [35]	Parallel plate-plate (Cr-Si)	Micromechanical resonant cavity	$\sim 15\%$
R. S. Decca et al. (2003, 2005) [36]	Sphere-plane	Micromechanical torsion oscillator (MEMS)	$\sim$ $0.2\% - 1.0\%$
J. N. Munday et al. (2009) [37]	Sphere-plane (in liquid)	AFM (Repulsive force in bromobenzene)	$\sim 5\%$
A. O. Sushkov et al. (2011) [38]	Sphere-plane (large distance)	Torsion balance (large-scale thermal effects)	$\sim 2\% - 5\%$

positioned at a distance a from the first, parallel to it, with $0 < a < L$ [5, 40], creating regions I and II. Furthermore, we will consider another configuration that will allow us to eliminate the divergence later: the plate is placed at a greater distance L/η so that in this position it does not experience the presence of the wall, and the energy in that region resembles that of a space without nearby boundaries, giving rise to regions III and IV. The Casimir energy is then defined as[17, 40]:

$$E_C(a) = \lim_{\eta \to \infty} \left\{ [E_I(a) + E_{II}(L-a)] - \left[E_{III}(L/\eta) + E_{IV}\left(L - \frac{L}{\eta}\right) \right] \right\} \tag{3.1}$$

3.1.1 Boundary conditions and permitted modes

Since the plates are perfectly conductive, then the following must be true [30]:

$$E_t|_S = B_n|_S = 0 \tag{3.2}$$

This structure allows us to decompose Maxwell's vector problem into two decoupled scalar problems: the condition on E_t gives rise to the transverse-electric (TE) modes, associated with a scalar function with a Dirichlet boundary condition, while the condition on B_n gives rise to the transverse-magnetic (TM) modes, associated with a scalar

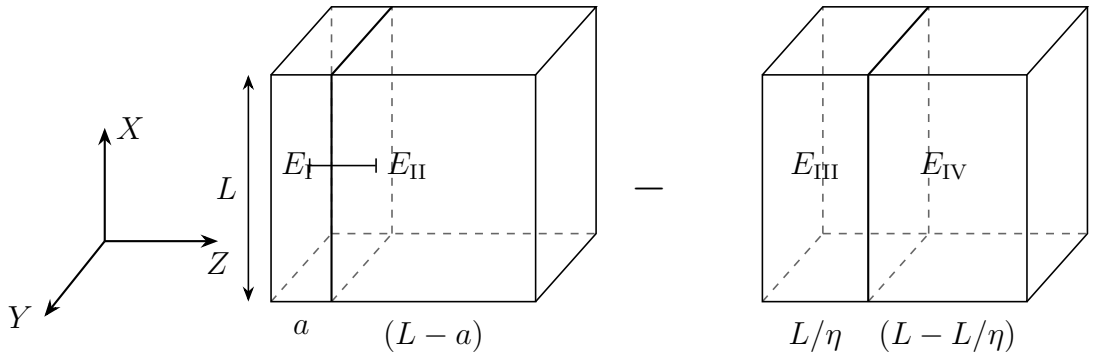


Figure 3.1: Subtraction of zero-point energies.

function with a von Neumann boundary condition. With this established, the problem reduces to solving the wave equation [40]:

$$\nabla^2\Phi - \frac{1}{c^2}\frac{\partial^2\Phi}{\partial t^2} = 0 \tag{3.3}$$

By searching for stationary solutions of the form $\Phi(\mathbf{r},t) = \Phi(\mathbf{r})e^{-i\omega t}$, the Helmholtz equation is obtained:

$$\nabla^2\Phi(\mathbf{r}) + \frac{\omega^2}{c^2}\Phi(\mathbf{r}) = 0 \tag{3.4}$$

Because the cavity has dimensions L, L and a, separating the variables in Cartesian coordinates allows us to write:

$$\Phi(x,y,z) = X(x)Y(y)Z(z) \tag{3.5}$$

We substitute into the Helmholtz equation Eq.(3.4):

$$\frac{1}{X}\frac{d^2X}{dx^2} + \frac{1}{Y}\frac{d^2Y}{dy^2} + \frac{1}{Z}\frac{d^2Z}{dz^2} + \frac{\omega^2}{c^2} = 0$$

Each term must be a constant:

$$\frac{1}{X}\frac{d^2X}{dx^2} = -k_x^2 \quad , \quad \frac{1}{Y}\frac{d^2Y}{dy^2} = -k_y^2 \quad , \quad \frac{1}{Z}\frac{d^2Z}{dz^2} = -k_z^2 \tag{3.6}$$

$$\frac{\omega^2}{c^2} = k_x^2 + k_y^2 + k_z^2 \tag{3.7}$$

The boundary conditions for the TM and TE modes determine the allowed values of k_z, while for the other directions, quantization is imposed by the cavity walls. Therefore, for the TM modes, the Dirichlet condition implies:

$$\Phi = 0 \quad \rightarrow \quad Z(z) = \sin(k_z z), \quad k_z = \frac{n\pi}{a}, \quad n = 1,2,3,\ldots \tag{3.8}$$

For TE modes, the Von Neumann condition implies:

$$\partial_z \Phi = 0 \quad \Rightarrow \quad Z(z) = \cos(k_z z), \quad k_z = \frac{n\pi}{a}, \quad n = 0, 1, 2, \ldots \tag{3.9}$$

For x and y:

$$k_x = \frac{\pi}{L} n_x \quad , \quad k_y = \frac{\pi}{L} n_y \tag{3.10}$$

Therefore, the frequencies for a given value of $\mathbf{k}_\parallel$ and an integer n are:

$$\omega_{n,k_\parallel} = \sqrt{k_\parallel^2 + \left(\frac{n\pi}{a}\right)^2} \tag{3.11}$$

Where $k_\parallel^2 = k_x^2 + k_y^2$

Recall that the plates are much larger compared to their separation (a), we take the $\lim L \to \infty$, at this limit the separation between consecutive modes has zero:

$$\Delta k_x = \frac{\pi}{L} \to 0 \quad , \quad \Delta k_y = \frac{\pi}{L} \to 0 \tag{3.12}$$

Approximation sum of rectangles

$$\sum_n f(x_n) \Delta x \approx \int f(x)\, dx$$

Thus, the discrete sum becomes an integral:

$$\sum_{n_x, n_y} \to \frac{L^2}{(2\pi)^2} \int_{-\infty}^{\infty} \int_{-\infty}^{\infty} dk_x\, dk_y = \frac{L^2}{(2\pi)^2} \int d^2 k_\parallel \tag{3.13}$$

Where $d^2 k_\parallel = dk_x\, dk_y$, the factor $L^2/(2\pi)^2$ is the density of states in wave space.

3.1.2 Zero-point energy

The zero point energy of the electromagnetic field in a vacuum is the sum of the energies $\frac{1}{2}\hbar\omega$ of all modes [41]:

$$E_I(a) = \frac{\hbar}{2} \sum \omega_{n,k_\parallel} \tag{3.14}$$

The total energy within this region of volume $L^2 a$ is then:

$$E_I(a) = \left(\frac{L}{2\pi}\right)^2 \int d^2 k_\parallel \sum_n g_n \frac{1}{2} \hbar \omega_n(k_\parallel) \tag{3.15}$$

Where g_n is the number of polarization states. For $n \geq 1$ we have two independent polarizations for the TE and TM modes, and for $n = 0$ there is only the TE mode, so $g_0 = 1$, thus for the terms $n \geq 1$ [42]:

$$\frac{1}{2}g_n\omega_n(k_\parallel) = \frac{1}{2}\cdot(2)\cdot\sqrt{|k_\parallel|^2+\left(\frac{n\pi}{a}\right)^2} = \sqrt{|k_\parallel|^2+\left(\frac{n\pi}{a}\right)^2} \tag{3.16}$$

and for $n = 0$:

$$\frac{1}{2}g_0\omega_0(k_\parallel) = \frac{1}{2}\cdot(1)\cdot\sqrt{|k_\parallel|^2+0} = \frac{1}{2}|k_\parallel| \tag{3.17}$$

Adding both modes together we get:

$$= \frac{1}{2}|k_\parallel|+\sum_{n=1}^{\infty}\sqrt{|k_\parallel|^2+\left(\frac{n\pi}{a}\right)^2} \tag{3.18}$$

Substituting in (3.15):

$$E_I(a) = \left(\frac{L}{2\pi}\right)^2\int d^2k_\parallel\left\{\frac{1}{2}|\mathbf{k}_\parallel|+\sum_{n=1}^{\infty}\sqrt{k_\parallel^2+\left(\frac{n\pi}{a}\right)^2}\right\} \tag{3.19}$$

Since the integrand depends only on the magnitude $k_\parallel = |\mathbf{k}_\parallel|$, then the system has rotational symmetry and to simplify the calculations, we can convert the two-dimensional integral $\int d^2k_\parallel$ to polar coordinates:

$$d^2k_\parallel = k_\parallel dk_\parallel d\theta \tag{3.20}$$

Since there is no angular dependence θ, the integral over the angle simply gives us a factor of 2π:

$$\int d^2k_\parallel = 2\pi\int_0^\infty k_\parallel dk_\parallel \tag{3.21}$$

Substituting in Eq.(3.19), we get:

$$E_T(a) = \frac{L^2}{2\pi}\int_0^\infty k_\parallel dk_\parallel\left\{\frac{1}{2}|\mathbf{k}_\parallel|+\sum_{n=1}^{\infty}\sqrt{k_\parallel^2+\left(\frac{n\pi}{a}\right)^2}\right\} \tag{3.22}$$

However, both the sum and the integral diverge when $k_\parallel \to \infty$, for the first term of the integral.

Evaluating this integral at a large upper limit Λ:

$$\int_0^\infty k_\parallel\left(\frac{1}{2}k_\parallel\right)dk_\parallel = \frac{1}{2}\int_0^\infty k_\parallel^2 dk_\parallel \tag{3.23}$$

$$\lim_{\Lambda\to\infty}\left[\frac{k_\parallel^3}{6}\right]_0^\Lambda = \lim_{\Lambda\to\infty}\frac{\Lambda^3}{6}\to\infty \tag{3.24}$$

Now for the second term (modes $n \geq 1$) for a $k_\parallel$ that is very large, we can approximate the square root as:

$$\sqrt{k_{\parallel}^2 + \left(\frac{n\pi}{a}\right)^2} \approx k_{\parallel} \tag{3.25}$$

Therefore:

$$\int_0^{\infty} k_{\parallel} \left(\sqrt{k_{\parallel}^2 + \left(\frac{n\pi}{a}\right)^2}\right) dk_{\parallel} \approx \int_0^{\infty} k_{\parallel}^2 dk_{\parallel} \to \infty \tag{3.26}$$

We can conclude that in the expression above we have two types of divergence: ultraviolet divergence and divergence in summation. One physical interpretation could be that the electrons on the surface of the plates cannot react quickly enough to cancel the fields, becoming transparent to these waves. However, a physical interpretation for this is not possible, given that we are dealing with extremely high frequencies [40].

3.1.3 Regularization

Regularization is a method used particularly in quantum field theory to deal with infinities or divergences that appear in calculations. It consists of a regulator or cutoff that allows these quantities to be finite and well-defined. Therefore, to correct this, we introduce a cutoff function $f(k/k_c)$ that decreases rapidly for values $k > k_c$, where k_c denotes the cutoff wavenumber, which we will assume to be of the order of the inverse of the atomic size and can define according to the condition $f(1) = \frac{1}{2}$. The simplest solution is an exponential cutoff as [40, 43]. For the first term $(n = 0)$

$$\frac{1}{2}|\mathbf{k}_{\parallel}| \to \frac{1}{2}|\mathbf{k}_{\parallel}| f\left(\frac{|\mathbf{k}_{\parallel}|}{k_c}\right) \tag{3.27}$$

For the second term $(n \geq 1)$

$$\left[k_{\parallel}^2 + \left(\frac{n\pi}{a}\right)^2\right]^{1/2} \to \left[k_{\parallel}^2 + \left(\frac{n\pi}{a}\right)^2\right]^{1/2} f\left(\frac{\left[k_{\parallel}^2 + \left(\frac{n\pi}{a}\right)^2\right]^{1/2}}{k_c}\right) \tag{3.28}$$

To calculate the Casimir energy, we must perform energy subtraction, since the energy of a single cavity depends on the artificial cut k_c. Recall that a is a small distance compared to that of cavities II $(L-a)$, III (L/n), and IV (L/n). Therefore, as with the modes in k_x and k_y, the separation of the modes k_z becomes infinitely small; again, the discrete sum becomes an integral. Additionally, it is important to note that the mode $n = 0$ is negligible for a large cavity, so the energy can be approximated as [40, 44]:

$$E_{\text{Big}} \approx \left(\frac{L}{2\pi}\right)^2 \int d^2 k_{\parallel} \left[\frac{D}{\pi} \int_0^{\infty} dk_z \, k_f(k/k_c)\right] \tag{3.29}$$

Where $D = (L-a) - \frac{L}{n} - \left(L - \frac{L}{n}\right)$

$$+\frac{1}{2\pi}\left((L-a)-\frac{L}{n}-\left(L-\frac{L}{n}\right)\right)\int dk_z\, f(k/k_c) \tag{3.30}$$

> **Note**
> The factor $1/\pi$ comes from the conversion from sum to integral with $1/2$ which is associated with the extension of the integral of k_z over the entire real axis.

Combining all the expressions, we obtain:

$$\begin{aligned} E(a,k_c) = \left(\frac{L}{2\pi}\right)^2 \int d^2k_\parallel \Bigg\{ & \frac{1}{2}|\mathbf{k}_\parallel| f\left(\frac{|\mathbf{k}_\parallel|}{k_c}\right) \\ & + \sum_{n=1}^{\infty}\left[k_\parallel^2+\left(\frac{n\pi}{a}\right)^2\right]^{1/2} f\left(\frac{\left[k_\parallel^2+\left(\frac{n\pi}{a}\right)^2\right]^{1/2}}{k_c}\right) \\ & + \frac{1}{2\pi}\left[(L-a)-\frac{L}{\eta}-\left(L-\frac{L}{\eta}\right)\right]\int dk_z\, f\left(\frac{k_z}{k_c}\right)\Bigg\} \end{aligned} \tag{3.31}$$

We can simplify this equation by taking the third term for energy:

$$(L-a)-\frac{L}{n}-\left(L-\frac{L}{n}\right) = L-a-\frac{L}{n}-L+\frac{L}{n} = -a \tag{3.32}$$

Substituting into the expression Eq. (3.31) we obtain:

$$\begin{aligned} E(a,k_c) = \left(\frac{L}{2\pi}\right)^2 \int d^2k_\parallel \Bigg\{ & \frac{1}{2}|\mathbf{k}_\parallel| f\left(\frac{|\mathbf{k}_\parallel|}{k_c}\right) \\ & + \sum_{n=1}^{\infty}\left[k_\parallel^2+\left(\frac{n\pi}{a}\right)^2\right]^{1/2} f\left(\frac{\left[k_\parallel^2+\left(\frac{n\pi}{a}\right)^2\right]^{1/2}}{k_c}\right) \\ & - \frac{a}{2\pi}\int_{-\infty}^{\infty} dk_z\, f\left(\frac{k_z}{k_c}\right)\Bigg\}. \end{aligned} \tag{3.33}$$

We again changed the integral to polar coordinates because when combining both expressions, the two-dimensional integral reappeared.

$$E(a,k_c) = \frac{L^2}{2\pi}\int_0^\infty k_\parallel\, dk_\parallel \Bigg\{ \frac{1}{2}k_\parallel f\left(\frac{k_\parallel}{k_c}\right) + \sum_{n=1}^{\infty}\sqrt{k_\parallel^2 + \left(\frac{n\pi}{a}\right)^2}\, f\left(\frac{\sqrt{k_\parallel^2+\left(\frac{n\pi}{a}\right)^2}}{k_c}\right) + \frac{a}{2\pi}\int_{-\infty}^{\infty} dk_z\, f\left(\frac{k_z}{k_c}\right)\Bigg\}. \tag{3.34}$$

We introduce a change of variable to unify the integrands:

$$y = \frac{a^2k_\parallel^2}{\pi^2} + n^2 \quad \text{and} \quad k_\parallel dk_\parallel = \frac{\pi^2}{2a^2}dy \tag{3.35}$$

so

$$E(a,k_c) = \frac{L^2\pi^2}{4a^3}\Bigg\{ \frac{1}{2}\int_0^\infty \sqrt{y}\, dy\, f\Big(\frac{\pi}{ak_c}\sqrt{y}\Big) + \sum_{n=1}^{\infty}\int_{n^2}^{\infty}\sqrt{y}\, dy\, f\Big(\frac{\pi}{ak_c}\sqrt{y}\Big)\Bigg\} - \int_0^\infty dn\int_{n^2}^{\infty}\sqrt{y}\, dy\, f\Big(\frac{\pi}{ak_c}\sqrt{y}\Big). \tag{3.36}$$

We will define a new auxiliary function in order to have a more compact equation:

$$F(n) = \int_{n^2}^{\infty} dy\sqrt{y}\, f\left(\frac{\pi}{ak_c}\sqrt{y}\right) \tag{3.37}$$

And if we evaluate at $n = 0$:

$$F(0) = \int_0^{\infty} dy\sqrt{y}\, f\left(\frac{\pi}{ak_c}\sqrt{y}\right) \tag{3.38}$$

Substituting (3.37) and (3.38) into (3.36) we obtain:

$$E(a,k_c) = \frac{L^2\pi^2}{4a^3}\left\{\frac{1}{2}F(0) + \sum_{n=1}^{\infty}F(n) - \int_0^\infty dnF(n)\right\} \tag{3.39}$$

The terms within the parentheses can be evaluated using the Euler-Maclaurin formula and the asymptotic behavior subject to the cutoff function[40].

Euler-Maclaurin Formula

The Euler-Maclaurin formula relates integrals to series. This formula can be used to approximate integrals by finite sums or vice versa [45].

$$\sum_{k=1}^{n-1} f_k = \int_0^n f(x)dx - \frac{1}{2}[f(0)+f(n)] + \sum_{k=1}^{\infty} \frac{B_{2k}}{(2k)!}\left[f^{(2k-1)}(n) - f^{(2k-1)}(0)\right] \quad (3.40)$$

Where B_{2k} denotes the Bernoulli numbers.

To adapt this formula to our problem, we must make the upper limit tend to infinity ($n \to \infty$), which results in:

$$\frac{1}{2}F(0) + \sum_{n=1}^{\infty} F(n) - \int_0^{\infty} F(x)dx = -\sum_{k=1}^{\infty} \frac{B_{2k}}{(2k)!}F^{(2k-1)}(0)$$

So, energy now takes the form of

$$E(a,k_c) = -\frac{L^2\pi^2}{4a^3}\sum_{k=1}^{\infty}\frac{1}{(2k)!}B_{2k}F^{(2k-1)}(0) \quad (3.41)$$

To derive this integral whose lower limit depends on the variable (n^2), we use Leibniz's rule.

Leibniz's Integral Rule

Leibniz's integral rule provides a formula for differentiating a definite integral [46].

$$\frac{d}{dn}\int_{a(n)}^{b(n)} g(y,n)dy = g(b(n),n)b'(n) - g(a(n),n)a'(n) + \int_{a(n)}^{b(n)} \frac{\partial g}{\partial n}(y,n)dy$$

Here $a(n) = n^2$, and $b(n) = \infty$.Replacing

$$F'(n) = 0 - g(n^2,n)\cdot(2n) + 0 = -2n\cdot\sqrt{n^2}\cdot f\left(\frac{\pi}{\alpha k_c}\sqrt{n^2}\right) \quad (3.42)$$

Simplifying $\sqrt{n^2} = |n|$.
If $n \geq 0$, then $|n| = n$.

$$F'(n) = -2n^2 f\left(\frac{\pi n}{\alpha k_c}\right) \quad (3.43)$$

After m derivatives ($m \geq 3$):

$$F^{(m)}(n) = -2\left[(m-1)(m-2)f^{(m-3)}\left(\frac{\pi n}{\alpha k_c}\right) + 2(m-1)nf^{(m-2)}\left(\frac{\pi n}{\alpha k_c}\right) + n^2 f^{(m)}\left(\frac{\pi n}{\alpha k_c}\right)\right] \quad (3.44)$$

Evaluating at zero

$$F^{(m)}(0) = -2(m-1)(m-2)f^{(m-3)}(0) \tag{3.45}$$

With $m = 2k - 1$:

$$F^{(2k-1)}(0) = -2(2k-2)(2k-3)f^{(2k-4)}(0) \tag{3.46}$$

We now substitute Eq. (3.46) into the general equation (3.41):

$$E(a, k_c) = -\frac{L^2\pi^2}{4a^3}\sum_{k=2}^{\infty}\frac{1}{(2k)!}B_{2k}\left[-2(2k-2)(2k-3)f^{(2k-4)}(0)\right] \tag{3.47}$$

Since the function depends on (π/ak_c), each time we differentiate with respect to n, this factor will appear; if we differentiate $(2k-4)$ times:

$$f^{(2k-4)}(0) = \left(\frac{\pi}{ak_c}\right)^{2k-4} C_{2k-4} \tag{3.48}$$

Donde C_{2k-4} es el valor numérico de esa derivada pura evaluada en cero. Sustituyendo en la Eq. (3.47):

$$E(a, k_c) = -\frac{L^2\pi^2}{4a^3}\sum_{k=2}^{\infty}\frac{1}{(2k)!}B_{2k}\left[-2(2k-2)(2k-3)\left(\frac{\pi}{ak_c}\right)^{2k-4} C_{2k-4}\right] \tag{3.49}$$

$$E(a, k_c) = \frac{L^2\pi^2}{2a^3}\sum_{k=2}^{\infty}\frac{1}{(2k)!}B_{2k}(2k-2)(2k-3)\left(\frac{\pi}{ak_c}\right)^{2k-4} C_{2k-4} \tag{3.50}$$

3.1.4 Casimir's Energy and Force

Physically, the cutoff constant is an artificial constant; we must remove the filter by making the cutoff tend to infinity, $k_c \to \infty$. Consequently, the terms in the summation from $k = 3$ onwards vanish, and only $k = 2$ survives.Thus $B_4 = -1/30$, $(2k)! = 24$ and $C_0 = 1$[40].

$$E_c(a) = \frac{L^2\pi^2}{2a^3} \times \left(-\frac{1}{360}\right) = -\frac{L^2\pi^2}{720}\frac{1}{a^3} \tag{3.51}$$

The equation above is the Casimir Energy in region I. To find the force exerted on the plates, we must differentiate the energy with respect to the separation distance:

$$F = -\frac{\partial E_c(a)}{\partial a} \tag{3.52}$$

To find the force per unit area (same as always), we divide the total force by the area of the plates, which is L^2:

$$F_c(a) = \frac{F}{L^2} = -\frac{1}{L^2}\frac{\partial E_c(a)}{\partial a} \tag{3.53}$$

$$F_c(a) = -\frac{\pi^2}{240}\frac{1}{a^4} \tag{3.54}$$

The negative sign indicates that it is an attractive force.

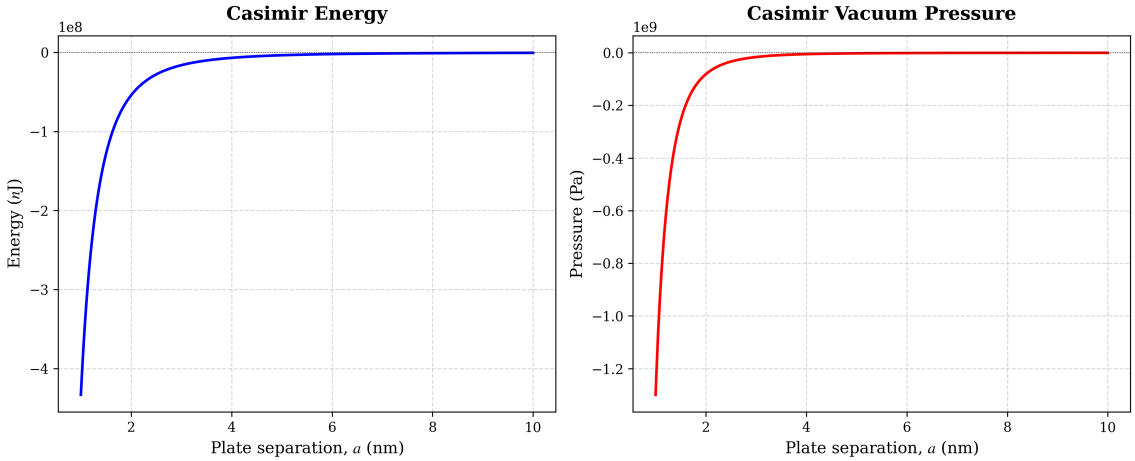


Figure 3.2: Behavior Casimir's Energy and Force for two parallel plane plates

3.2 Two Concentric Spheres

This section develops the calculation of the Casimir effect between two concentric spheres with boundary conditions $\psi_{\omega\ell m} = (a, \theta, \phi) = 0$ and $\psi_{\omega\ell m} = (b, \theta, \phi) = 0$ whose separation distance is $b - a = d$ [47].

We start with the spacetime metric:

$$ds^2 = dt^2 - (dr^2 + r^2 d\theta^2 + r^2 \sin^2\theta d\phi^2) \tag{3.55}$$

where $\theta \in [0, \pi]$ and $\phi \in [0, 2\pi]$. The wave equation that the massless scalar field satisfies in these coordinates is given by

$$\Box\Psi(t, r, \theta, \phi) = 0$$

$$\Box\Psi = -\partial_t^2\Psi + \frac{1}{r^2}\partial_r(r^2\partial_r\Psi) + \frac{1}{r^2\sin\theta}\partial_\theta(\sin\theta\partial_\theta\Psi) + \frac{1}{r^2\sin^2\theta}\partial_\phi^2\Psi = 0 \tag{3.56}$$

We assume that the total wave function can be factored into a temporal part, a radial part, and an angular part:

$$\Psi(t, r, \theta, \phi) = T(t)R(r)Y(\theta, \phi) \tag{3.57}$$

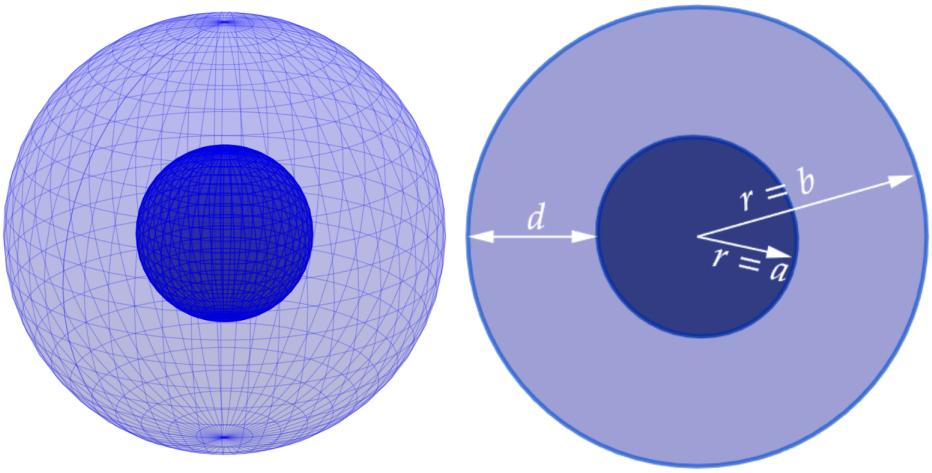


Figure 3.3: Geometry representation of the system, two concentric spheres of radius a and b, qith a sepatation distance d.

Replacing this proposal into the wave equation Eq. (3.56) and dividing by $\Psi = TRY$:

$$-\frac{1}{T}\frac{d^2T}{dt^2} + \frac{1}{R}\frac{1}{r^2}\frac{d}{dr}\left(r^2\frac{dR}{dr}\right) + \frac{1}{Y}\frac{1}{r^2}\Lambda^2 Y = 0 \tag{3.58}$$

Temporal solution

- The equation is separated into a time and space part, resulting in the separation constant $-\omega^2$, therefore, the resulting time equation is:

$$\frac{d^2T}{dt^2} + \omega^2 T = 0 \tag{3.59}$$

Its solution is a combination of complex exponentials, taking the form:

$$T(t) \propto e^{-i\omega t} \tag{3.60}$$

Angular and Radial Separation

By substituting the time constant into the space equation and separating variables, the angular equation of the spherical harmonics is obtained:

$$\Lambda^2 Y(\theta,\phi) + \ell(\ell+1)Y(\theta,\phi) = 0 \tag{3.61}$$

The solution is the spherical harmonics:

$$Y(\theta,\phi) = Y_{\ell m}(\theta,\phi) = Ne^{im\phi}P_\ell^m(\cos\theta) \tag{3.62}$$

The radial part satisfies:

$$r^2\frac{d^2R}{dr^2} + 2r\frac{dR}{dr} + \left[\omega^2r^2 - \ell(\ell+1)\right]R = 0 \tag{3.63}$$

By the change of variable $R(r) = r^{-1/2}u(r)$, it is transformed into the Bessel equation of order $\nu = \ell + \frac{1}{2}$:

$$r^2u'' + ru' + \left[\omega^2r^2 - \left(\ell+\frac{1}{2}\right)^2\right]u = 0 \tag{3.64}$$

The general radial solution is:

$$R(r) = r^{-1/2}\left[A_\ell J_{\ell+1/2}(\omega r) + B_\ell N_{\ell+1/2}(\omega r)\right] \tag{3.65}$$

The complete solution is a superposition over all modes (ℓ, m) and frequencies ω:

$$\Psi_{\omega\ell m}(t,r,\theta,\phi) = \sum_{\omega,\ell,m} e^{-i\omega t}r^{-1/2}\left[A_\ell J_{\ell+1/2}(\omega r) + B_\ell N_{\ell+1/2}(\omega r)\right]Y_{\ell m}(\theta,\phi) \tag{3.66}$$

3.2.1 Boundary Conditions

To find the form of the boundary coefficients, we apply the boundary conditions:

$$\Psi_{\omega\ell m}(t, r=a, \theta, \phi) = 0 \tag{3.67}$$

$$\Psi_{\omega\ell m}(t, r=b, \theta, \phi) = 0 \tag{3.68}$$

From the condition at $r = a$:

$$B_\ell = -A_\ell\frac{J_{\ell+1/2}(\omega a)}{N_{\ell+1/2}(\omega a)} \tag{3.69}$$

The condition at $r = b$ leads to the equation that determines the allowed frequencies ω:

$$J_{\ell+1/2}(\omega b)N_{\ell+1/2}(\omega a) - J_{\ell+1/2}(\omega a)N_{\ell+1/2}(\omega b) = 0 \tag{3.70}$$

This equation quantizes the values of ω for each ℓ, it's known as the transcendental equation.

Bessel Polynomials [48]

First kind:

$$J_n(x) = \sum_{k=0}^{\infty}\frac{(-1)^k(x/2)^{n+2k}}{k!\,(n+k)!} \tag{3.71}$$

Second kind:

$$Y_n(x) = \frac{J_n(x)\cos(n\pi) - J_{-n}(x)}{\sin(n\pi)} \tag{3.72}$$

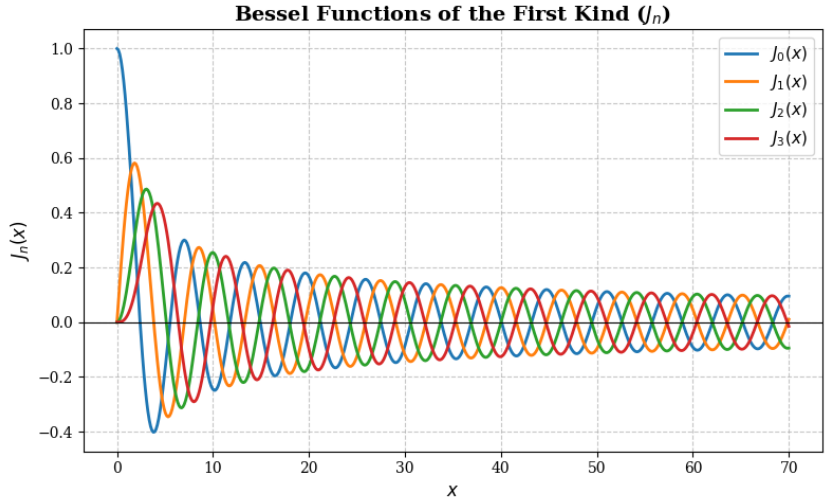


Figure 3.4: Behavior of the Besse Funtions of the First kind

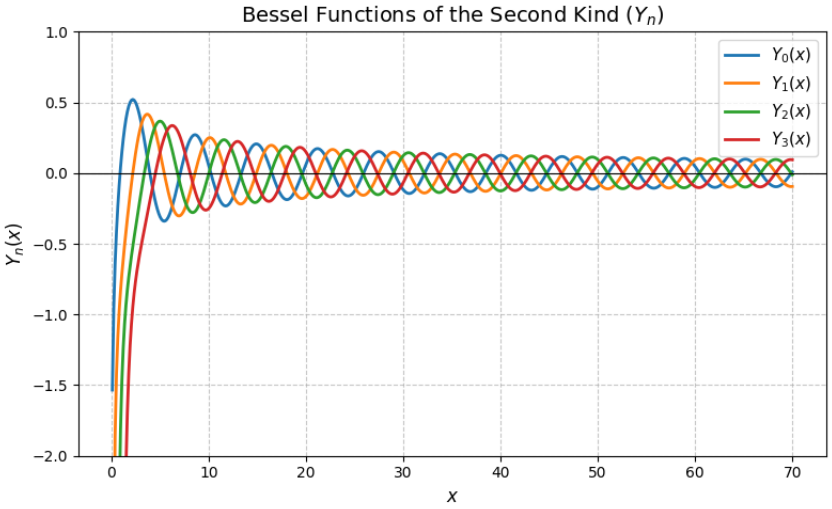


Figure 3.5: Behavior of the Besse Funtions of the Second kind.

The Casimir energy for the massless scalar field between two concentric spheres is:

$$E_C = \frac{\hbar}{2}\sum\omega = \frac{\hbar}{2}\sum_{\ell=0}^{\infty}\sum_{m=-\ell}^{\ell}\sum_{n=1}^{\infty}\omega_{n\ell} \tag{3.73}$$

The frequencies depend explicitly on ℓ and m. Since the space is spherical, it does not have a preferred angular direction, which leads to a degeneracy with respect to m:

$$E_C = \frac{1}{2}\sum_{\ell=0}^{\infty}(2\ell+1)\sum_{n=1}^{\infty}\omega_{n\ell} = \sum_{\ell=0}^{\infty}\nu\sum_{n=1}^{\infty}\omega_{n\ell} \quad \text{with} \quad \ell+\frac{1}{2}=\nu \tag{3.74}$$

Where the eigenfrequencies $\omega_{n\ell}$ are determined by solving the transcendental equation. We note that Bessel functions are defined as an infinite power series in x. Although Bessel series converge for any value, when $|x|$ is very large, they converge very slowly. Even though the series has slow convergence, the initial terms of said series do not provide information about the sum. To overcome this difficulty, we need to evaluate the fast convergence, which means that the series rapidly approaches a constant when $\omega \to \infty$. For this, it is proposed to use asymptotic expansions [47].

Then, the Casimir energy defined by the eigenfrequency spectrum for fixed arguments ℓ and large order as $\ell \to \infty$ is:

$$E_C = \sum_{\ell=0}^{\infty} \nu \sum_{n=1}^{\infty} \omega_{n\ell} \to \sum_{\ell=0}^{\infty} \nu \sum_{n=1}^{\infty} \tilde{\omega}_{n\ell} \tag{3.75}$$

$\tilde{\omega}$ is a solution of Bessel's equation:

$$z^2 \frac{d^2y}{dz^2} + z\frac{dy}{dz} + (z^2 - \nu^2)y = 0 \tag{3.76}$$

To obtain $z = \tilde{\omega}a \gg 1$, a change of variable is made that removes the $1/z$ term of the first derivative, as it complicates the analysis.

For large arguments $x = \tilde{\omega}a \gg 1$ and fixed order ν, the behavior of Bessel functions $J_\nu(x)$ and Neumann functions $N_\nu(x)$ is studied using the asymptotic expansions of Hankel functions.

Hankel Functions

Hankel functions of the first and second order are defined as linear combinations of $J_\nu(x)$ and $N_\nu(x)$:

$$H_\nu^{(1)}(x) = J_\nu(x) + iN_\nu(x) \tag{3.77}$$

$$H_\nu^{(2)}(x) = J_\nu(x) - iN_\nu(x) \tag{3.78}$$

For $x \gg 1$:

$$H_\nu^{(1)}(x) \sim \sqrt{\frac{2}{\pi x}}\, e^{i\left(x - \frac{\nu\pi}{2} - \frac{\pi}{4}\right)} \left[P(\nu, x) + iQ(\nu, x)\right] \tag{3.79}$$

Where $P(\nu, x)$ and $Q(\nu, x)$ are asymptotic expansions of the form:

$$P(\nu, x) = 1 - \frac{(\mu - 1)(\mu - 9)}{2!\,(8x)^2} + \ldots \tag{3.80}$$

$$Q(\nu, x) = \frac{\mu - 1}{8x} - \frac{(\mu - 1)(\mu - 9)(\mu - 25)}{3!\,(8x)^3} + \ldots \tag{3.81}$$

Where $\mu = 4\nu^2$ is the Hankel parameter. Now, focusing on a first-order approximation in $1/x$ and substituting $e^{ix} = \cos x + i \sin x$, the Hankel function yields:

$$H_\nu^{(1)}(x) \approx \sqrt{\frac{2}{\pi x}} \left(\cos\chi + i \sin\chi\right) \left[P(\nu, x) + iQ(\nu, x)\right] \tag{3.82}$$

with $\chi = x - \frac{\nu\pi}{2} - \frac{\pi}{4}$.

From the Hankel functions, $J_\nu(x)$ and $N_\nu(x)$ are directly obtained:

$$J_\nu(x) = \mathrm{Re}\left[H_\nu^{(1)}(x)\right] \tag{3.83}$$

$$N_\nu(x) = \mathrm{Im}\left[H_\nu^{(1)}(x)\right] \tag{3.84}$$

Thus, for $J_\nu(x)$:

$$J_\nu(x) \approx \sqrt{\frac{2}{\pi x}}\left[P(\nu,x)\cos\chi - Q(\nu,x)\sin\chi\right] \tag{3.85}$$

Substituting $\chi = x - \frac{\nu\pi}{2} - \frac{\pi}{4}$ for $x = \tilde{\omega}a - \frac{\nu\pi}{2} - \frac{\pi}{4}$:

$$J_\nu(\tilde{\omega}a) \approx \sqrt{\frac{2}{\pi\tilde{\omega}a}}\left[\cos\left(\tilde{\omega}a - \frac{\nu\pi}{2} - \frac{\pi}{4}\right) - \frac{(4\nu^2-1)}{8\tilde{\omega}a}\sin\left(\tilde{\omega}a - \frac{\nu\pi}{2} - \frac{\pi}{4}\right)\right] \tag{3.86}$$

And taking the imaginary part:

$$N_\nu(\tilde{\omega}a) \approx \sqrt{\frac{2}{\pi\tilde{\omega}a}}\left[\sin\left(\tilde{\omega}a - \frac{\nu\pi}{2} - \frac{\pi}{4}\right) + \frac{(4\nu^2-1)}{8\tilde{\omega}a}\cos\left(\tilde{\omega}a - \frac{\nu\pi}{2} - \frac{\pi}{4}\right)\right] \tag{3.87}$$

Taking the leading zero-order approximation of the equations:

$$J_\nu(x) \approx \sqrt{\frac{2}{\pi x}}\cos\left(x - \frac{\nu\pi}{2} - \frac{\pi}{4}\right) \quad \text{and} \quad N_\nu(x) \approx \sqrt{\frac{2}{\pi x}}\sin\left(x - \frac{\nu\pi}{2} - \frac{\pi}{4}\right) \tag{3.88}$$

Substituting into the transcendental equation:

$$\sqrt{\frac{2}{\pi\tilde{\omega}a}}\cos\chi(\tilde{\omega}a)\cdot\sqrt{\frac{2}{\pi\tilde{\omega}b}}\sin\chi(\tilde{\omega}b) - \sqrt{\frac{2}{\pi\tilde{\omega}b}}\cos\chi(\tilde{\omega}b)\cdot\sqrt{\frac{2}{\pi\tilde{\omega}a}}\sin\chi(\tilde{\omega}a) = 0 \tag{3.89}$$

Factoring out $\frac{2}{\pi\tilde{\omega}\sqrt{ab}}$ and using the trigonometric identity $\sin(A-B) = \sin A\cos B - \cos A\sin B$, we obtain:

$$\sin\left(\chi(\tilde{\omega}b) - \chi(\tilde{\omega}a)\right) = 0 \tag{3.90}$$

We observe that the phase difference is $\tilde{\omega}(b-a)$.

Therefore:

$$\sin(\tilde{\omega}(b-a)) = 0 \implies \tilde{\omega}(b-a) = n\pi \quad \text{with} \quad (n = 1,2,3,\dots) \tag{3.91}$$

which gives us $\tilde{\omega} = \frac{n\pi}{b-a}$. Now, including the second-order frequency correction [47]:

$$\tilde{\omega}_{n\ell} \approx \left(\frac{n\pi}{b-a}\right)^2 + \frac{\nu^2}{ab} \quad \text{where} \quad n = 1,2,3,4,5,6,\dots \tag{3.92}$$

In order for the separation between shells to remain fixed even if the dimensions change, the equation is rewritten in terms of a dimensionless variable $\lambda = \frac{b}{a} > 1$, and the frequency argument is scaled[47].

$$f_\ell(vw,\lambda) = J_\nu(vw)N_\nu(vw\lambda) - J_\nu(vw\lambda)N_\nu(vw) = 0$$

where $w = wa/v$

Thus, the form for the energy becomes:

$$E_c = \sum_{\ell=0}^{\infty} \nu \sum_{n=1}^{\infty} w_{n\ell} + \sum_{\ell=0}^{\infty} \nu \sum_{n=1}^{\infty} \sqrt{\left(\frac{n\pi}{b-a}\right)^2 + \frac{\nu^2}{ab}}$$

3.2.2 Regularization Method

Given that the n gives an infinite summation, we introduce a regular $e^{-\alpha w_n}$ where $\alpha \to 0$

For the first part of the energy:

$$\bar{E}_c = \sum_{\ell=0}^{\infty} \left(\ell + \frac{1}{2}\right) \sum_{n=1}^{\infty} w_{n\ell}$$

Defining the internal sum of frequency for a ℓ:

$$S_\ell = \sum_{\ell=0}^{\infty} \left(\ell + \frac{1}{2}\right) S_\ell \quad \to \quad \bar{E}_c = \sum_{\ell=0}^{\infty} \left(\ell + \frac{1}{2}\right) S_\ell$$

This exponential regulator suppresses high-frequency models. Since we do not know the closed form of $w_{n\ell}$, we cannot directly add term by term. To solve this, it is plausible to use Cauchy's theorem. The zeros of the analytic function on the real axis will be exactly the eigenfrequencies of $w_{n\ell}$ [47].

$$\overline{E}_C = -\frac{1}{\pi b} \lim_{\alpha\to 0} \sum_{l=0}^{\infty} \nu \,\mathrm{Re}\, e^{-i\phi} \int_0^\infty dy\, e^{-i\alpha y e^{-i\phi}/b} y \frac{d}{dy} \ln f_\nu(\nu y e^{-i\phi}, \lambda) \tag{3.93}$$

Deforming the contour C towards the imaginary axis ($z = -iande^{-i\phi}$ with $\phi \to 0$) and taking the real part, the sum becomes the integral Using Lommel's multiplication theorem for Bessel functions, to calculate the integrals [47], the result we obtain is

$$= i\,(-1)^{n+1} \frac{(2n)!\; v^{2n}}{(2n)!} \left(\frac{b}{a}\right)^{2n+1} \tag{3.94}$$

It is observed that all terms are purely imaginary, but for it to be physical, its real part must be extracted, therefore:

$$\bar{E}_c = 0 \tag{3.95}$$

Therefore, the modes $\ell \to \infty$ do not contribute to the energy. This means that the entire energy contribution is given by

$$\tilde{E}_c = \sum_{\ell=0}^{\infty} \nu \sum_{n=1}^{\infty} \sqrt{\left(\frac{n\pi}{b-a}\right)^2 + \frac{\nu^2}{ab}} \tag{3.96}$$

Abel-Planar Formula

$$\sum_{n=1}^{\infty} f(n) - \int_0^{\infty} f(x)dx = \frac{1}{2}f(0) + i\int_0^{\infty} \frac{f(it) - f(-it)}{e^{2\pi t} - 1}dt \tag{3.97}$$

For the regularization treatment we use the Abel-Plana formula.
We fix ℓ and identify $f(n)$ as $\sqrt{\left(\frac{n\pi}{d}\right)^2 + \frac{\nu^2}{db}}$, in this order $f(0) = \sqrt{\frac{\nu^2}{ab}} = \frac{\nu}{\sqrt{ab}}$

$$\tilde{E}_C = -\frac{1}{2\sqrt{ab}}\sum_{l=0}^{\infty}\nu^2 - 2\sum_{l=0}^{\infty}\nu\int_{\frac{\nu\xi}{2\pi}}^{\infty}\left[\left(\frac{t\pi}{d}\right)^2 - \frac{\nu^2}{ab}\right]^{1/2}\frac{dt}{e^{2\pi t} - 1} \tag{3.98}$$

The first divergent term is regularized by the Hurwitz Zeta function $\zeta(s, q)$

$$\sum_{l=0}^{\infty}\left(l + \frac{1}{2}\right)^2 = \zeta\left(-2, \frac{1}{2}\right) = 0 \tag{3.99}$$

We are left with the sum over ℓ of the function $F(\nu)$:

$$\tilde{E}_C = -2\sum_{l=0}^{\infty}F(\nu), \quad F(\nu) = \nu\int_{\frac{\nu\xi}{2\pi}}^{\infty}\left[\left(\frac{t\pi}{d}\right)^2 - \frac{\nu^2}{ab}\right]^{1/2}\frac{dt}{e^{2\pi t} - 1} \tag{3.100}$$

The integral of $F(x)$ produces the dominant term:

$$\int_0^{\infty} F(x)dx = \frac{1}{8\pi}\frac{ab}{d^3}\zeta(4) \tag{3.101}$$

Therefore, the total Casimir energy results in [47]:

$$E_C = -\frac{1}{4\pi}\frac{ab}{d^3}\zeta(4)\left[1 + \frac{1}{12}\eta^2\frac{\zeta(2)}{\zeta(4)}\right] \tag{3.102}$$

Substituting the zeta functions $\zeta(4) = \frac{\pi^4}{90}$ and $\zeta(2) = \frac{\pi^2}{6}$, we arrive at:

$$E_C = -\frac{\pi^3}{360}\frac{ab}{d^3}\left[1 + \frac{5}{4\pi^2}\frac{d^2}{ab}\right] \tag{3.103}$$

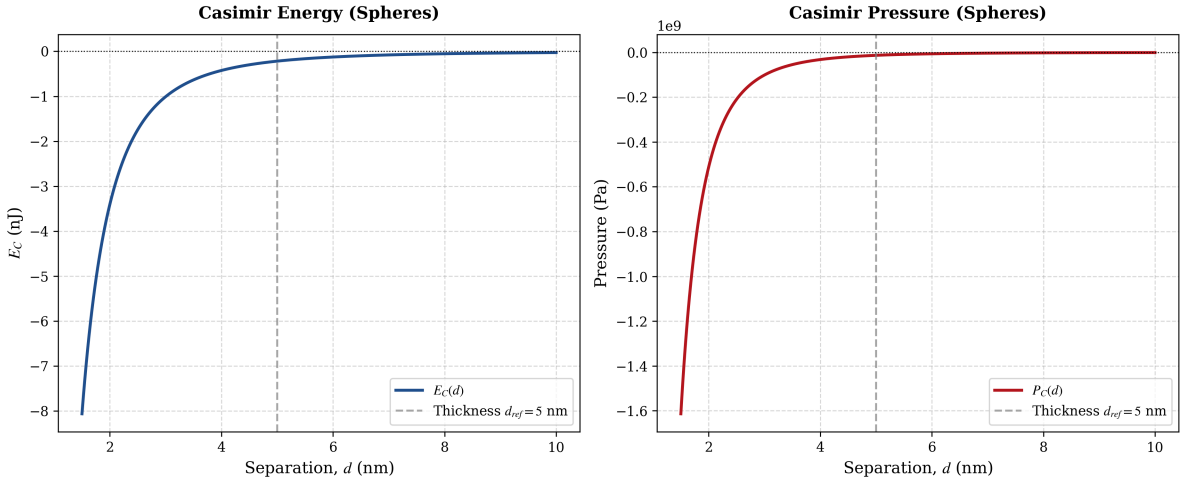


Figure 3.6: Casimir energy and associated pressure for a spherical geometry. Dependence of the Casimir energy $E_C(d)$ (left, in nJ) and Casimir pressure $P_C(d)$ (right, in Pa) on the separation distance d ranging from 1.5 nm to 10 nm. The geometric parameters were set to $a \approx 10\ \mu\text{m} - 5$ nm) and $b = 10\ \mu$m. Both magnitude curves exhibit the characteristic attractive (negative) behavior of the Casimir force, increasing nonlinearly as the separation approaches sub-10 nm regimes. A reference distance $d_{\text{ref}} = 5$ nm is highlighted by the vertical dashed line.

4

The Lipid Membrane as a Boundary System for the Casimir Effect

4.1 Biological Membranes

A living cell consists of a plasma membrane and the set of molecules that self-replicate within it. This first part has a simple structure, consisting of a sheet of lipid molecules approximately 5 nm thick, and acts as a barrier that prevents the cell's contents from escaping, but at the same time allows the selective entry of substances. This process is a necessary condition for the cell to survive. This controlled permeability is due to transport proteins and other biomolecules, which act as molecular sensors that respond to changes in their environment. Regarding the mechanical properties of the membrane, when a cell grows or undergoes deformation, its membrane is modified, increasing its surface area without losing its continuity. Even in cases where it has been perforated, it does not collapse, but rather rapidly self-repairs to maintain its structural integrity [1].

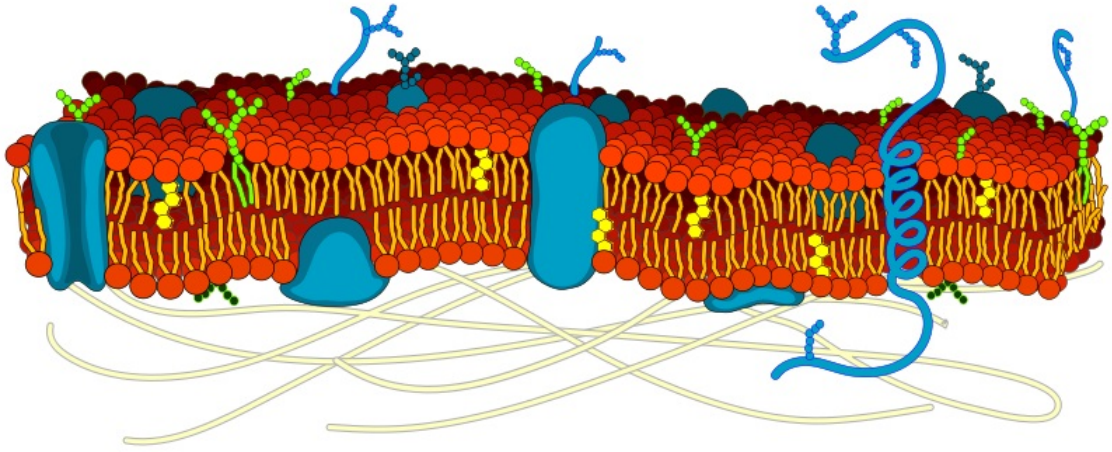


Figure 4.1: Schematic representation of a biological membrane with a lipid bilayer. Retrieved from: https://biomodel.uah.es/model2/lip/membranas-func.htm

4.2 Lipid Membranes

The characteristics of the lipid bilayer are largely responsible for the properties of the cell membrane. The lipids of the bilayer have a hydrophilic head and one or two hydrophobic tails. The most abundant type of lipid in the membrane are phospholipids, and in particular dipalmitoylphosphatidylcholine (DPPC) lipids, widely used in biophysical studies (See Figure 4.2). These DPPC lipids are called amphipathic molecules and endow the membrane with the following characteristics: fluidity, selective permeability, and the ability to undergo phase transitions between gel and liquid-crystalline states, modulated by factors such as temperature and the presence of cholesterol [1, 2].

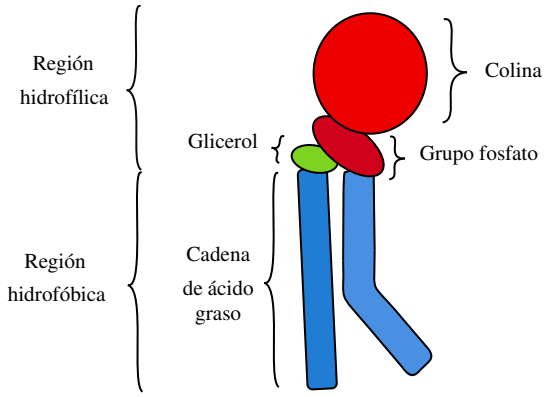


Figure 4.2: General structure of a dipalmitoylphosphatidylcholine molecule. The polar head is composed of a choline group attached to a phosphate, while the hydrophobic region corresponds to two long hydrocarbon chains, which constitute the lipid "tails." Source: Author's own work

4.2.1 Membrane Potential

Membrane potential (V_m) is defined as the potential difference between the inside of the membrane (V_i) and the outside (V_e). This potential is a direct result of the unequal distribution of ions and also of the selective permeability of the membrane. Fig. 4.3 shows two compartments separated by a membrane selectively permeable to $\mathtt{K}^+$. Since the concentration of $\mathtt{K}^+$ is 10 times greater in compartment 2 than in compartment 1, there is a tendency for $\mathtt{K}^+$ to move from compartment 2 to compartment 1. Consequently, and because $\mathtt{Cl}^-$ is not permeable, electroneutrality is disrupted, generating a concentration gradient of the ionic species in both compartments, which ultimately results in an electrical potential [49].

In a less ideal biological system, non-diffusible ions, such as macromolecules with a net negative charge, can be introduced into the model. Their presence also marks an asymmetry in the ion distribution. These immobile species generate a Gibbs-Donnan effect, which describes the electrochemical equilibrium that the system must reach to

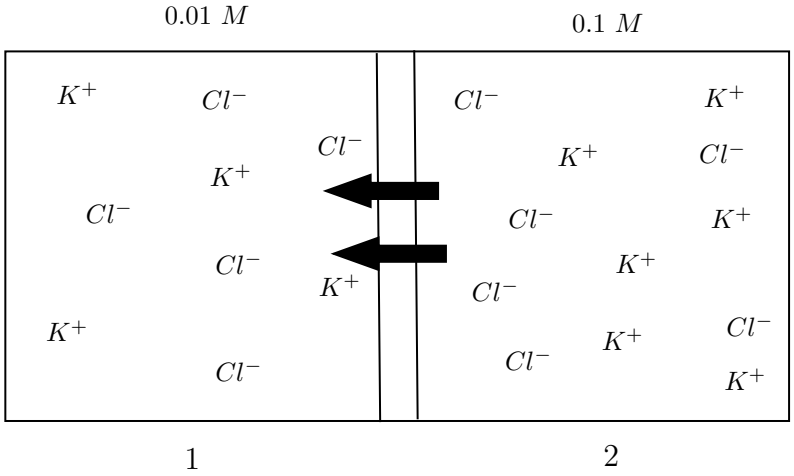


Figure 4.3: Compartment separated by a membrane where ions are driven from 2 to 1 as a result of chemical and electrical power differences. Source: Own elaboration

maintain electroneutrality. In the case of a cell, the membrane potential takes on values that are not equilibrium values. This implies a system with energy expenditures that would allow the cell to maintain a steady state [49].

Under physiological conditions, the membrane is simultaneously permeable to the different ionic species present. Therefore, it must be considered that the potential does not correspond to the equilibrium of a single species but to a weighted equilibrium of the different species. This is described by the Goldman-Hodgkin-Katz equation [49].

$$\Delta V = \frac{RT}{F} \ln \left(\frac{p_{\mathtt{K}}[\mathtt{K}]_1 + p_{\mathtt{Na}}[\mathtt{Na}]_1 + p_{\mathtt{Cl}}[\mathtt{Cl}]_2}{p_{\mathtt{K}}[\mathtt{K}]_2 + p_{\mathtt{Na}}[\mathtt{Na}]_2 + p_{\mathtt{Cl}}[\mathtt{Cl}]_1} \right) \tag{4.1}$$

Where R and F are constants, p is the selective permeability. From a thermodynamic point of view, the membrane potential reflects a dynamic electrochemical state, in which the chemical and electrical components of the free energy partially compensate for each ionic species. On the other hand, from a physicochemical point of view, it reflects a steady state maintained by concentration gradients that require energy [49].

4.2.2 Equivalent electrical circuit for a biological membrane

Capacitors are passive electrical components that store energy in the form of an electrostatic field; typically, their traditional structure consists of two conductive plates separated by a dielectric material. The maximum energy a capacitor can store depends on these two factors [50]. Similarly, the lipid bilayer can be modeled as a parallel-plate capacitor. In this image, we can associate the capacitor plates with the polar heads of the lipids located at both ends of the membrane, and as an insulating material, we associate their fatty acid chains, forming a dielectric medium of low relative permittivity. Meanwhile, the intracellular and extracellular compartments function as ionic

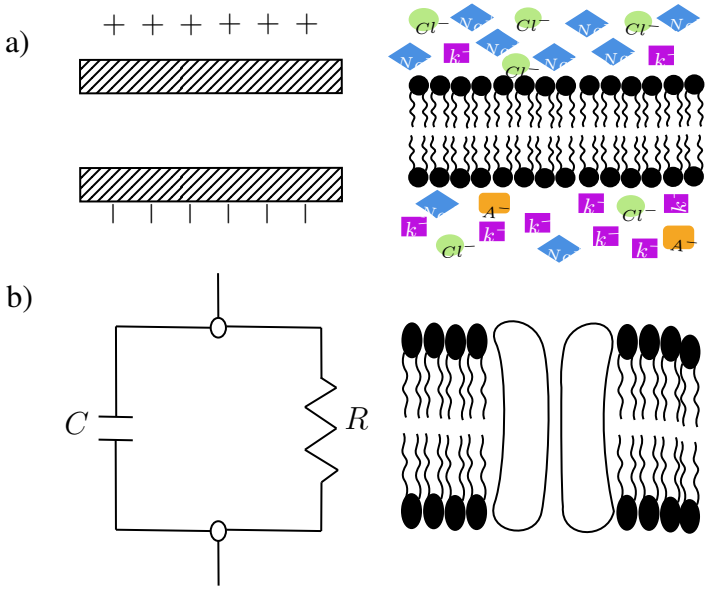


Figure 4.4: Diagram of a cell membrane and its equivalent circuit. a) The lipid bilayer acts as a charge storage device, like a capacitor. b) Model of a membrane and transport protein, where the capacitor represents the membrane, and the resistance (R) models the ionic conductance due to the transport channels. Source: Author's own work

conductors. Together, this configuration allows the accumulation of charge of different signs on both sides of the membrane, enabling the emergence of a membrane potential [49].

4.3 Viability of the Casimir effect

As shown in Section 4.2, the asymmetric distribution of ionic species across the bilayer—maintained by selective permeability and described by the Goldman-Hodgkin-Katz equation—generates a membrane potential ΔV. This electrochemical asymmetry is what allows the lipid bilayer to be represented, as a first approximation, as a parallel-plate capacito: the polar heads of the lipids act as the two charged plates, the hydrocarbon tails act as the dielectric core, and the intra/extracellular media act as the ionic conductors on either side. It is important to be explicit about what this analogy does and does not license. The capacitor description is a classical electrostatic picture, while the Casimir effect is a quantum electrodynamic vacuum phenomenon; the two do not share a physical mechanism. What they do share is a geometric configuration: two extended, parallel, closely spaced surfaces. It is precisely this shared geometry and not a shared physical origin, that motivates this analysis: treating the bilayer, as a working hypothesis, as if it were the pair of parallel plates of the canonical Casimir problem, in order to test whether a vacuum boundary contribution of the right order of magnitude and the right distance-dependence could plausibly coexist with the electrostatic picture

already established.

Geometric validity: parallel plates vs. spherical caps

Before opting for the parallel-plate geometry, it must be justified rather than assumed, given that a cell is topologically a sphere rather than an infinite sheet. For this reason, this work also solves the Casimir problem for two concentric spherical shells (Section 3.2); the spherical boundary-value problem is solved directly, without local approximation as a flat surface, and the large-radius limit is examined only subsequently.

Take the cell radius as $R \approx 10\mu$ an the membrane thicknees as $d \approx 5nm$, so that R is 2000 times larger than the bilayer thikness. The relevant dimensionless curvature parametes is:

$$h = \frac{d}{R} = 5 \times 10^{-4} \tag{4.2}$$

The leading curvature correction to the spherical Casimir energy. relative to flat parallel-plate result, is

$$\frac{5}{4\pi^2}\frac{d^2}{ab} \approx 3.16 \times 10^{-8} \tag{4.3}$$

This correction is smaller by roughly seven orders of magnitude than unity, which means that, at the cellular scale, the spherical geometry is mathematically indistinguishable from the plane-parallel limit. This is also consistent with the fact that we are working with a scalar field carrying a single polarization degree of freedom in the spherical (Dirichlet) calculation; once the electromagnetic case is reconstructed by including both TE and TM contributions, the energy density is exactly double the scalar result,

$$\frac{E_C}{A}\Big|_{EM} = 2 \times \Big(-\frac{\pi^2}{1440 d^3}\Big) = -\frac{\pi^2}{730 d^3} \tag{4.4}$$

This exactly reproduces the coefficient obtained independently for the electromagnetic field between two parallel plates in Section 3.1.4. This cross-verification allows the $\pi^2/1440$ coefficient from the calculation for concentric spheres (scalar, Dirichlet) to be reconciled with the $\pi^2/720$ coefficient from the calculation for flat plates (electromagnetic), rather than treating them as two disconnected results.

- **On the role of the Bessel functions:** The reason the curvature correction vanishes so rapidly is evident in the behavior of the special functions appearing in the transcendental equation (3.70). For a system the size of a single cell, the physically relevant modes correspond to a very high multipole order, $\ell \sim b/d \gg 1$. In this regime, the exact Bessel/Neumann functions J_ν, N_ν (Figs. 3.4–3.5) are well described by Debye's uniform asymptotic expansions, and the eigenfrequency spectrum collapses into the simple form $\tilde{\omega}_{n\ell} \approx (n\pi/(b-a))^2 + \nu^2/(ab)$ derived in Eq. (3.92): the curvature-dependent term $\nu^2/(ab)$ is parametrically suppressed relative to the plate-like term $(n\pi/(b-a))^2$ precisely when $d \ll R$. In other words,

the oscillatory and rapidly converging nature of the Bessel function arguments ensures that the mode sum is dominated by the flat-space contribution, and it is this, rather than an ad hoc approximation, that justifies neglecting the spherical-cap correction.

Casimir pressure vs. Hamaker pressure

With the flat-plate geometry justified, the ideal (perfect-conducto, $T = 0$) Casimir pressure at the membran thickness $d = 5nm$ is

$$P_C = \frac{\pi^2 \hbar c}{240 d^4} \approx 2.08 \times 10^6 Pa \tag{4.5}$$

To assess whether this vacuum contribution is negligible or competitive with known membrane interactions, it is compared against the Hamaker force, the classical, non-retarded van der Waals interaction between macroscopic bodies, obtained by pairwise summation of molecular dispersion interactions rather than from field quantization. For two parallel slabs it gives a pressure

$$P_{Hamaker} = \frac{A_H}{6\pi d^3} \tag{4.6}$$

Where A_H is the Hamaker constant, of order $A_H 10^{-20}$ for lipid bilayers in an aqueos medium. Ealuated at $d = 5nm$:

$$P_{Hamaker} \approx 4.24 \times 10^3 Pa \tag{4.7}$$

Therefore, the two pressures differ by approximately two or three orders of magnitude, with the estimate for the ideal vacuum exceeding the classical estimate (which omits retardation effects) at this separation distance. This should not be interpreted as proof that the Casimir effect dominates interactions between real membranes: both figures represent idealized limits (perfect conductors in one case and undamped pairwise dispersion forces in the other), and neither constitutes an accurate model of the actual dielectric response of a lipid bilayer. What the comparison does demonstrate is that the vacuum contribution is not automatically negligible compared to a conventional van der Waals estimate at this length scale; for precisely this reason, that value is subsequently compared with the measured mechanical rigidity of a real membrane.

4.3.1 Transverse compressibility modulus

A reference point with a more solid physical basis than Hamaker's estimate is the membrane's own measured mechanical response. The transverse (out-of-plane) compressibility modulus associated with any pressure law $P(d)$ is defined as the system's elastic response to compression:

$$K_\perp = -d\frac{\partial P}{\partial d} \tag{4.8}$$

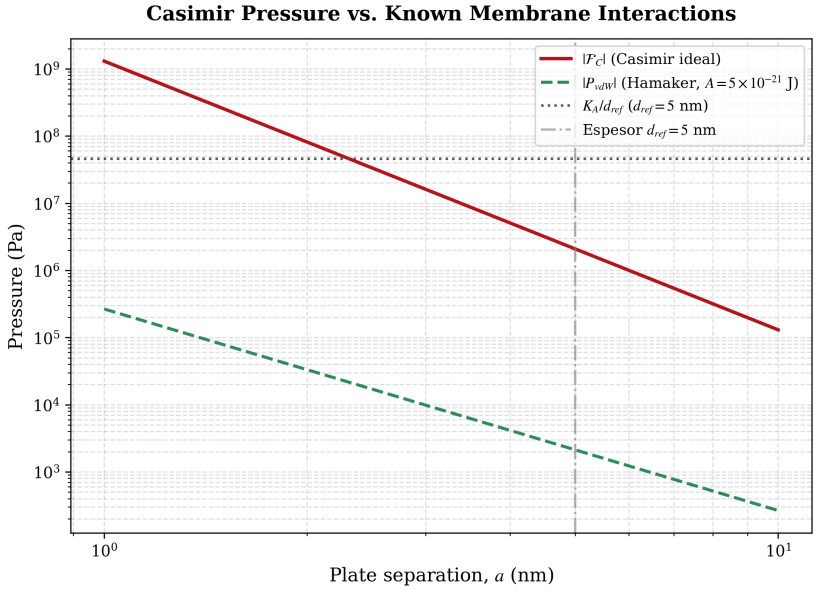


Figure 4.5: Comparison between Casimir pressure and Hamaker pressure

For the ideal Casimir pressure, which scales as $P \propto d^{-4}$, this gives $K_\perp = P$, so that at $d = 5nm$, with a perfect-conductor boundary at $T = 0K$

$$K_\perp^{Casimir} \approx 8.32 \times 10^6 Pa \tag{4.9}$$

The transverse compresibility modulus reported in the biophysicall literature for real lipied bilayer is of order

$$K_\perp^{realbilayer} \approx 1.7 \times 10^9 Pa \tag{4.10}$$

The ratio between the two is

$$\frac{K_\perp^{realbilayer}}{K_\perp^{Casimir}} \approx 204 \tag{4.11}$$

This is the central quantitative result of the feasibility analysis: the purely electromagnetic vacuum, under the idealization of perfect conductors, exerts a restoring pressure approximately 204 times lower than that required to explain, on its own, the transverse rigidity of a real bilayer. Therefore, the Casimir effect contributes to the mechanical description of the membrane but does not, from a mechanical standpoint, account for the stabilization of the bilayer at its characteristic thickness of 5 nm.

Thermal validity: the Matsubara criterion

All of the above assumes the strict zero-temperture limit. At finite temperature T, the continuous frequancy integral of the vacuum energy is replaced by a discerete sum over Matsubra frequencies,

$$\varepsilon_n = \frac{2\pi k_B T}{\hbar} n, \qquad n = 1, 2, 3, ... \tag{4.12}$$

and the $T = 0$ treatment used throughout this thesis us valid only while the membrane thickness is much smaller than the thermal wavelength

$$d_T = \frac{\hbar c}{2\pi k_B T} \tag{4.13}$$

At physiological temperature, $T = 310K$:

$$d_T \approx 1.18\mu m \tag{4.14}$$

Comparing this to the membrane thickness:

$$\frac{d}{d_T} \approx 4 \times 10^{-3} \tag{4.15}$$

Since the distance d is approximately 250 times smaller than the thermal wavelength, the temperature correction to the Casimir energy is negligible. Far from contradicting the conclusion of Section 4.3.4, this finding reinforces it: the nearly 200-fold difference between the ideal vacuum contribution and the membrane's actual stiffness is not an artifact arising from the neglect of temperature. Rather, it stems from a structural property of the idealized boundary conditions, suggesting that the missing physical key lies in the dielectric nature of the membrane rather than in thermal fluctuations.

Conclusion

This work evaluated the plausibility of the Casimir effect as a physical mechanism contributing to the organization of lipid membranes. The starting point was the observation that asymmetric ionic distributions impart a measurable membrane potential to the bilayer, naturally suggesting its representation as a parallel-plate capacitor. Although the electrostatic capacitor and the quantum electrodynamic vacuum do not share a physical mechanism, they do share the same parallel-plate geometry, which motivated the application of the Casimir theoretical framework to this system.

First, the geometric validity of this choice was established: by solving the Casimir problem directly for two concentric spherical shells and comparing the result with that for flat, parallel plates, it was demonstrated that the curvature correction at the cellular scale ($R \approx 10$ μm, $d \approx 5$ nm) is on the order of 10^{-8}—that is, negligible. This result, combined with the asymptotic (Debye) behavior of the Bessel functions governing the spherical mode spectrum for high multipole orders, justifies using the flat, parallel-plate configuration without the need for any correction factor.

Within this configuration, the ideal Casimir pressure was compared, firstly, with the classical Hamaker/van der Waals pressure (neglecting retardation effects) and, secondly, with the transverse compressibility modulus measured in a real bilayer. This

second comparison is decisive: the ideal vacuum contribution underestimates the actual membrane stiffness by a factor of approximately 204. The Matsubara criterion for finite temperatures confirms that this discrepancy is not a thermal artifact, as the membrane thickness is nearly 250 times smaller than the thermal wavelength at physiological temperature, placing the problem entirely within the $T = 0$ regime used in the calculation.

Taken all together, these results support the following interpretation of the Casimir effect as a model for membrane organization. The energy and force curves obtained for both studied geometries, i.e., parallel plates and concentric spheres—are strictly monotonic: they exhibit neither minima nor equilibrium points and, therefore, lack features that could explain on their own why a bilayer stabilizes at precisely the thickness it displays. In this sense, the model is an idealized proposal regarding feasibility rather than a mechanistic model: it neither reproduces the actual system nor predicts its characteristic length scale. What it does establish is that the bilayer geometry is compatible with a Casimir-like boundary contribution of plausible, albeit insufficient, magnitude. The persistent discrepancy—by a factor of approximately 200—between the prediction for an ideal vacuum and the actual mechanical modulus (a difference that remains after accounting for both curvature and thermal effects) is best attributed not to the quantum vacuum itself, but to the actual, finite dielectric response of the lipid material—an aspect that the idealized perfect-conductor boundary condition employed here fails to capture. This points directly to Lifshitz theory—incorporating the frequency-dependent permittivity of water and lipids—as the natural next step in transforming this argument for geometric feasibility into a quantitatively adequate physical model.

Bibliography

[1] Bruce Alberts, Dennis Bray, and Karen Hopkin. *Introducción a la biología celular*. Ed. Médica Panamericana, 2006.

[2] John Katsaras and Thomas Gutberlet. "Lipid bilayers: structure and interactions". In: (2013).

[3] Piotr H Pawlowski and Piotr Zielenkiewicz. "The quantum Casimir effect may be a universal force organizing the bilayer structure of the cell membrane". In: *The Journal of membrane biology* 246.5 (2013), pp. 383–389.

[4] Benjamin B Machta, Sarah L Veatch, and James P Sethna. "Critical Casimir forces in cellular membranes". In: *Physical review letters* 109.13 (2012), p. 138101.

[5] Hendrick BG Casimir. "On the attraction between two perfectly conducting plates". In: *Proc. Kon. Ned. Akad. Wet.* Vol. 51. 1948, p. 793.

[6] Paul Adrien Maurice Dirac. "The quantum theory of the emission and absorption of radiation". In: *Proceedings of the Royal Society of London. Series A, Containing Papers of a Mathematical and Physical Character* 114.767 (1927), pp. 243–265.

[7] Franz Mandl and Graham Shaw. *Quantum field theory*. John Wiley & Sons, 2013.

[8] Jun John Sakurai and Jim Napolitano. *Modern quantum mechanics*. Cambridge university press, 2020.

[9] Steven Weinberg. *The quantum theory of fields*. Vol. 2. Cambridge university press, 1995.

[10] Gerald D Mahan. *Many-particle physics*. Springer Science & Business Media, pag 1, 2013.

[11] Richard L Liboff. *Introductory quantum mechanics*. Pearson Education India, 2003.

[12] Harald JW Muller-Kirsten. *Introduction to quantum mechanics: Schrodinger equation and path integral*. World Scientific Publishing Company, 2012.

[13] Richard P Feynman, Albert R Hibbs, and Daniel F Styer. *Quantum mechanics and path integrals*. Courier Corporation, 2010.

[14] Claude Cohen-Tannoudji, Bernard Diu, and Franck Laloë. *Quantum Mechanics, Volume 1: Basic Concepts, Tools, and Applications*. 2nd. Weinheim: Wiley-VCH, 2019. ISBN: 978-3-527-34554-0.

[15] David J Griffiths and Darrell F Schroeter. *Introduction to quantum mechanics*. Cambridge university press, 2018.

[16] Max Born and Emil Wolf. *Principles of optics: electromagnetic theory of propagation, interference and diffraction of light*. Elsevier, 2013.

[17] Walter Greiner. *Quantum mechanics: an introduction*. Springer Science & Business Media, 2011.

[18] John David Jackson. *klassische Elektrodynamik*. Walter de Gruyter, 2013.

[19] Wolfgang Nolting. *Theoretical physics*. PUBDB-2017-153651. Springer, 2016.

[20] John David Jackson and Lev Borisovich Okun. "Historical roots of gauge invariance". In: *Reviews of modern physics* 73.3 (2001), p. 663.

[21] John David Jackson. "From Lorenz to Coulomb and other explicit gauge transformations". In: *American Journal of Physics* 70.9 (2002), pp. 917–928.

[22] AM Stewart. "Vector potential of the Coulomb gauge". In: *European journal of physics* 24.5 (2003), pp. 519–524.

[23] Franz Mandl. *Quantum mechanics*. John Wiley & Sons, 2013.

[24] Michael E Peskin. *An Introduction to quantum field theory*. CRC press, 2018.

[25] Christopher C Gerry and Peter L Knight. *Introductory quantum optics*. Cambridge university press, 2023.

[26] John David Jackson and Ronald F Fox. *Classical electrodynamics*. 1999.

[27] John M. Lee. *Introduction to Smooth Manifolds*. 2nd. Vol. 218. Graduate Texts in Mathematics. New York: Springer, 2012. Chap. 15.

[28] Hendrik BG Casimir and Dirk Polder. "The influence of retardation on the London-van der Waals forces". In: *Physical Review* 73.4 (1948), p. 360.

[29] Hendrik Brugt Gerhard Casimir and Hendrik Brugt Gerhard Casimir. *Haphazard reality: Half a century of science*. Amsterdam University Press, 2010.

[30] Michael Bordag, Umar Mohideen, and Vladimir M Mostepanenko. "New developments in the Casimir effect". In: *Physics reports* 353.1-3 (2001), pp. 1–205.

[31] Marcus J Sparnaay. "Measurements of attractive forces between flat plates". In: *Physica* 24.6-10 (1958), pp. 751–764.

[32] Peter HGM van Blokland and J Theodoor G Overbeek. "Van der Waals forces between objects covered with a chromium layer". In: *Journal of the Chemical Society, Faraday Transactions 1: Physical Chemistry in Condensed Phases* 74 (1978), pp. 2637–2651.

[33] Steven K Lamoreaux. "Demonstration of the Casimir force in the 0.6 to 6 μ m range". In: *Physical Review Letters* 78.1 (1997), p. 5.

[34] Umar Mohideen and Anushree Roy. "Precision measurement of the Casimir force from 0.1 to 0.9 μ m". In: *Physical Review Letters* 81.21 (1998), p. 4549.

[35] Giacomo Bressi et al. "Measurement of the Casimir force between parallel metallic surfaces". In: *Physical review letters* 88.4 (2002), p. 041804.

[36] RS Decca et al. "Measurement of the Casimir force between dissimilar metals". In: *Physical review letters* 91.5 (2003), p. 050402.

[37] Jeremy N Munday, Federico Capasso, and V Adrian Parsegian. "Measured long-range repulsive Casimir–Lifshitz forces". In: *Nature* 457.7226 (2009), pp. 170–173.

[38] AO Sushkov et al. "Observation of the thermal Casimir force". In: *Nature Physics* 7.3 (2011), pp. 230–233.

[39] Gerald E Marsh. "Quantum Fluctuations, The Casimir Effect and The Historical Burden". In: *arXiv preprint arXiv:2206.01865* (2022).

[40] Günter Plunien, Berndt Müller, and Walter Greiner. "The casimir effect". In: *Physics Reports* 134.2-3 (1986), pp. 87–193.

[41] Peter W Milonni and Mei-Li Shih. "Casimir forces". In: *Contemporary Physics* 33.5 (1992), pp. 313–322.

[42] Roger Balian and Bertrand Duplantier. "Geometry of the Casimir effect". In: *arXiv preprint quant-ph/0408124* (2004).

[43] Thorsten Emig. "Casimir forces and geometry in nanosystems". In: *Nonlinear Dynamics of Nanosystems* (2010), pp. 165–202.

[44] Andreson LC Rego, CA Linhares, and APC Malbouisson. "Casimir effect via a generalized Matsubara formalism". In: *arXiv preprint arXiv:1608.01367* (2016).

[45] Tom M. Apostol. "An Elementary View of Euler's Summation Formula". In: *The American Mathematical Monthly* 106.5 (1999), pp. 409–418. DOI: 10.2307/2589145.

[46] Milton Abramowitz and Irene A. Stegun, eds. *Handbook of Mathematical Functions with Formulas, Graphs, and Mathematical Tables*. 9th ed. p. 11. New York: Dover Publications, 1972.

[47] Mustafa Özcan. "Scalar Casimir effect between two concentric spheres". In: *International Journal of Modern Physics A* 27.16 (2012), p. 1250082.

[48] George B Arfken, Hans J Weber, and Frank E Harris. *Mathematical methods for physicists: a comprehensive guide*. Academic press, 2011.

[49] Mario Parisi. *Temas de biofísica*. Mc Graw Hill, 2004.

[50] Qi Li. *Advanced Dielectric Materials for Electrostatic Capacitors*. Institution of Engineering and Technology, 2020.